

Review

# Atomic Force Microscopy as a Tool to Study Transport Phenomena in Biological Systems

Sneha Kandapal  and Bingqian Xu \* 

Single Molecule Study Laboratory, College of Engineering and Nanoscale Science and Engineering Center, University of Georgia, Athens, GA 30602, USA; sneha.kandapal@uga.edu

\* Correspondence: nanoxu@uga.edu

**Abstract:** Biological interactions often involve the transport of molecules, ions, or other species across biological membranes or between interacting proteins. The understanding of these transport phenomena is crucial for the development of therapies for various diseases. Atomic force microscopy is a powerful tool that has been increasingly used to study biological systems at the nano scale. The high resolution, quantitative measurements, and the ability to probe biological interactions under near-physiological conditions make AFM an attractive tool for investigating transport phenomena in biological systems. In this article, we focus on the use of AFM in the study of the transport phenomena in biological systems. We discuss the principles of AFM, its instrumentation, and its application in the study of biomolecules and biological systems. We also provide a comprehensive overview of recent articles that have utilized AFM in the study of biomarkers in biological systems.

**Keywords:** atomic force microscopy; biomarkers; transport; binding interactions; physical properties; biological systems



**Citation:** Kandapal, S.; Xu, B. Atomic Force Microscopy as a Tool to Study Transport Phenomena in Biological Systems. *Processes* **2023**, *11*, 2430. <https://doi.org/10.3390/pr11082430>

Academic Editors: Kun Wang and Han Hu

Received: 12 May 2023

Revised: 18 July 2023

Accepted: 20 July 2023

Published: 12 August 2023



**Copyright:** © 2023 by the authors. Licensee MDPI, Basel, Switzerland. This article is an open access article distributed under the terms and conditions of the Creative Commons Attribution (CC BY) license (<https://creativecommons.org/licenses/by/4.0/>).

## 1. Introduction

Atomic force microscopy (AFM) [1,2] is a technique that is used not only for high-resolution imaging of a variety of materials, but also in the assessment of diverse physical characteristics at the nano scale. It finds extensive applications across various disciplines, including physics, chemistry, biology, and materials science, enabling the investigation of diverse physical and chemical properties at the molecular level. AFM [3] has equipped scientists with indispensable tools and resources to investigate the structure and properties of a wide range of samples, spanning from individual atoms to complex biological systems. These investigations hold broad applications, from fundamental research to industrial endeavors. Due to its remarkable capacity to deliver high-resolution images and precise measurements at the nano scale, it has emerged as an ever more crucial instrument in the examination of biosystems. This technology empowers researchers to visualize the surface of biological samples, enabling them to extract comprehensive data pertaining to topography, structure, and arrangement. Consequently, scientists can now delve into the intricate world of diverse biological molecules, such as proteins, DNA, RNA, and lipids [4–8], unraveling their structure–function relationships and gaining valuable insights. In addition it can serve as a valuable tool for investigating the mechanical characteristics of biological materials [9], such as their stiffness and elasticity, and provide insights into biomolecules and their role in biological processes such as cell adhesion [8,10], migration [11,12], and signaling [13,14]. With its remarkable ability to image and manipulate individual molecules, AFM has emerged as a potent instrument in the examination of isolated molecules, thereby offering invaluable insights into their behavior and function. This capability has revolutionized the study of biological molecules, including enzymes [15,16], receptors [17,18], and transporters [19,20].

AFM has proven highly valuable in the realm of investigating transport phenomena within biological systems. Transport phenomena involve the movement of particles or

molecules across media like cell membranes or tissue barriers. In-depth exploration of transport phenomena within biological interactions, encompassing molecular binding and recognition processes involving proteins, nucleic acids, and lipids, sheds light on fundamental biological processes such as cell adhesion, protein–protein interactions, and drug delivery. Diverse mechanisms drive these interactions, including electrostatic interactions, hydrogen bonding, van der Waals interactions, and hydrophobic interactions. AFM finds noteworthy applications in the study of transport phenomena, with a specific focus on studying the blood–brain barrier (BBB) [21,22]. Acting as a complex barrier, the BBB separates blood vessels from brain tissue and plays a vital role in regulating the transport of nutrients, ions, and other molecules into the brain. AFM has facilitated investigations into the mechanical properties of the BBB and the interactions between the BBB and circulating cells and molecules. By quantifying the local mechanical properties of the BBB, AFM offers insights into the barrier’s permeability and transport properties. Similarly, AFM has proven to be instrumental in studying transport phenomena in ion channels [23–26]. These membrane proteins govern ion flow across cell membranes and are pivotal in various biological processes, such as nerve impulse transmission and muscle contraction. The exploration of biomolecular interactions through AFM has unveiled valuable insights into a wide array of biological processes, holding potential for the development of novel therapies and diagnostic tools. This review delves into the diverse applications of AFM in studying transport phenomena within biological interactions.

## 2. Principles of AFM

AFM is a scanning probe microscopy technique that facilitates the measurement of the interaction between a probe (Figure 1) and a specimen surface [27]. The probe is affixed to a flexible cantilever and systematically moved across the sample surface in a controlled manner, where it experiences various forces, such as contact, electric, magnetic, electrostatic, and Van der Waals forces. The deflection of the cantilever is gauged using a laser beam, which is directed onto a position-sensitive detector after being reflected off the back of the cantilever. This deflection information is then utilized to compute the forces operating between the probe and the sample surface. AFM can operate in multiple modes, including contact mode, tapping mode, and non-contact mode. In contact mode, the tip continuously maintains contact with the sample surface, and the deflection data acquired generate a topographic image of the surface. In tapping mode, the tip oscillates near its resonance frequency, and the resulting deflection data are utilized to create a topographic image of the surface. In non-contact mode, the tip is brought close to the sample surface without contacting it. The interaction between the tip and the sample surface causes a shift in the resonance frequency of the cantilever, which is measured and exploited to generate a topographic image.

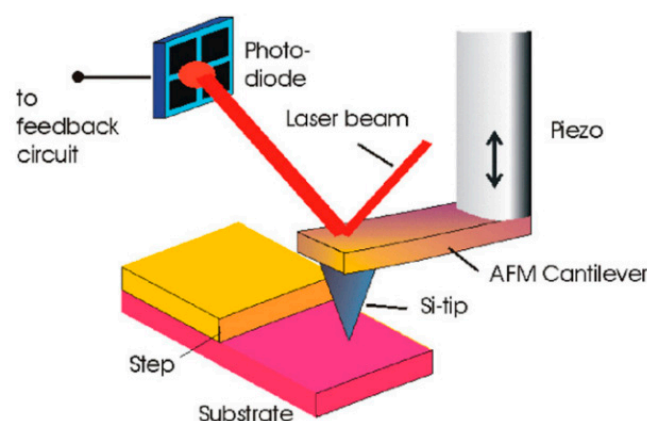


**Figure 1.** Schematic diagram showing the major components of an atomic force microscope with an optical beam deflection system. Reprinted with permission from [27].

### 2.1. Probe and Cantilever Design

The design of both the AFM probe and the cantilever plays a pivotal role in determining the resolution and sensitivity of the instrument. The AFM probe is composed of silicon or silicon nitride and features a sharp tip that scans across the sample surface. To enhance the detection of the cantilever's motion, the tip is often coated [28,29] with a reflective material. The design of the tip is critical in achieving high-resolution imaging. A sharp and well-defined tip enables the detection of small features on the specimen surface, whereas a blunt or irregular tip can result in poor resolution and inaccurate measurements. Additionally, the dimensions and geometry of the tip affect the interaction forces with the sample, thereby influencing the precision and sensitivity of the measurements. The cantilever, on the other hand, is a thin and flexible beam that provides support to the AFM probe and detects its deflection as it scans the sample surface. Like the AFM probe, the cantilever is typically made of silicon or silicon nitride and is coated with a reflective material to enhance the detection of its motion. The stiffness, length, and width of the cantilever all contribute to its resonant frequency, which determines the speed and accuracy of the measurements. It is crucial to match the resonant frequency of the cantilever with the frequency of the AFM feedback loop to achieve optimal performance [30,31]. Proper tuning ensures effective interaction between the cantilever and the sample surface, enabling precise and reliable measurements. There are many distinct types of AFM probes and cantilevers available, each with its own advantages and disadvantages. For example, the use of ultrathin cantilevers [32] can improve resolution and sensitivity but can also lead to increased noise and decreased stability. Similarly, the use of specialized probe coatings [33] can improve the detection of specific properties, such as magnetic or chemical properties, but can lead to increased tip wear and reduced probe lifetime. In conclusion, the design of the AFM probe and cantilever is critical for achieving high-resolution, high-sensitivity imaging in AFM. The choice of probe [34,35] and cantilever design should be based on the specific requirements of the experiment and the properties of the sample being investigated. By meticulously considering these variables, AFM becomes an instrumental tool for exploring the intricate properties of surfaces and materials at the nano scale.

### 2.2. Detection of Cantilever Deflection

The precise detection of cantilever deflection constitutes a pivotal aspect of AFM, enabling in-depth exploration of the nanoscale properties exhibited by surfaces and materials. The deflection of the cantilever is directly proportional to the interaction forces occurring between the probe and the specimen, serving as a potent tool for investigation. Among the various methods available for detecting cantilever deflection in AFM, optical detection [36] stands out as the most commonly utilized. In this approach, a laser beam is directed onto the cantilever, and the reflected light is captured by a photodetector. As the cantilever deflects, the position of the reflected beam undergoes changes, facilitating precise measurement of the cantilever's deflection. This method provides high sensitivity and excellent temporal resolution, allowing for real-time monitoring of the cantilever's position. Another method for detecting cantilever deflection is piezoresistive detection [37,38]. In this method, the cantilever is coated with a piezoresistive material that changes its electrical resistance as the cantilever deflects. This change in resistance can be measured by a Wheatstone bridge circuit, providing a direct measurement of the cantilever's deflection. Piezoresistive detection provides high sensitivity and is well suited for use in high-frequency AFM applications. Capacitive detection [39] is another method for detecting cantilever deflection in AFM. In this approach, the cantilever is positioned between two capacitive plates, and the alteration in capacitance resulting from the deflection of the cantilever is quantified. This method provides excellent linearity and sensitivity but is typically more complex and expensive than optical or piezoresistive detection. Finally, there are several specialized detection methods that have been developed for specific AFM applications. For instance, magnetic detection is utilized to identify the deflection of a magnetic cantilever in magnetic force microscopy (MFM), while thermal detection is employed to measure the deflection

of a thermally sensitive cantilever in thermal AFM applications. Thus, the detection of cantilever deflection is a critical aspect of AFM, and a variety of methods are available for achieving high sensitivity and accuracy.

### 2.3. Force Measurement

Force measurement using AFM is a highly effective technique for exploring the physical properties of materials [40]. The most widely used method for force measurement in AFM is force spectroscopy. In force spectroscopy, the cantilever is brought into contact with the sample surface and then gradually retracted at a constant velocity, while simultaneously measuring the deflection of the cantilever. The resulting force–distance curve (Figure 2) [41] provides valuable insights into the mechanical characteristics of the sample, including its stiffness, elasticity, surface roughness, adhesion, viscoelasticity, and plastic deformation. Force spectroscopy can be conducted with a variety of probe geometries, such as spherical, pyramidal, and conical tips, tailored to the specific experimental requirements. Another approach for force measurement in AFM is lateral force microscopy (LFM). In LFM [42], the cantilever is scanned across the sample while detecting the forces between the probe and the sample. This technique enables the investigation of frictional properties and the mapping of lateral force distributions across the sample. MFM represents a third method for force measurement. It employs a magnetic cantilever to measure the magnetic forces between the probe and the sample surface. It allows for the investigation of the magnetic properties of materials and the mapping of magnetic force distributions across the sample. Additionally, several specialized force measurement techniques have been developed for specific applications. These include electrostatic force microscopy (EFM), capacitance force microscopy (CFM), and nanoindentation. EFM is employed to investigate electrical properties, CFM is utilized to explore dielectric properties, and nanoindentation focuses on the mechanical properties of materials. Thus, force measurement using AFM presents a potent approach for examining the physical properties of materials and surfaces at the nano scale, enabling comprehensive characterization and analysis.

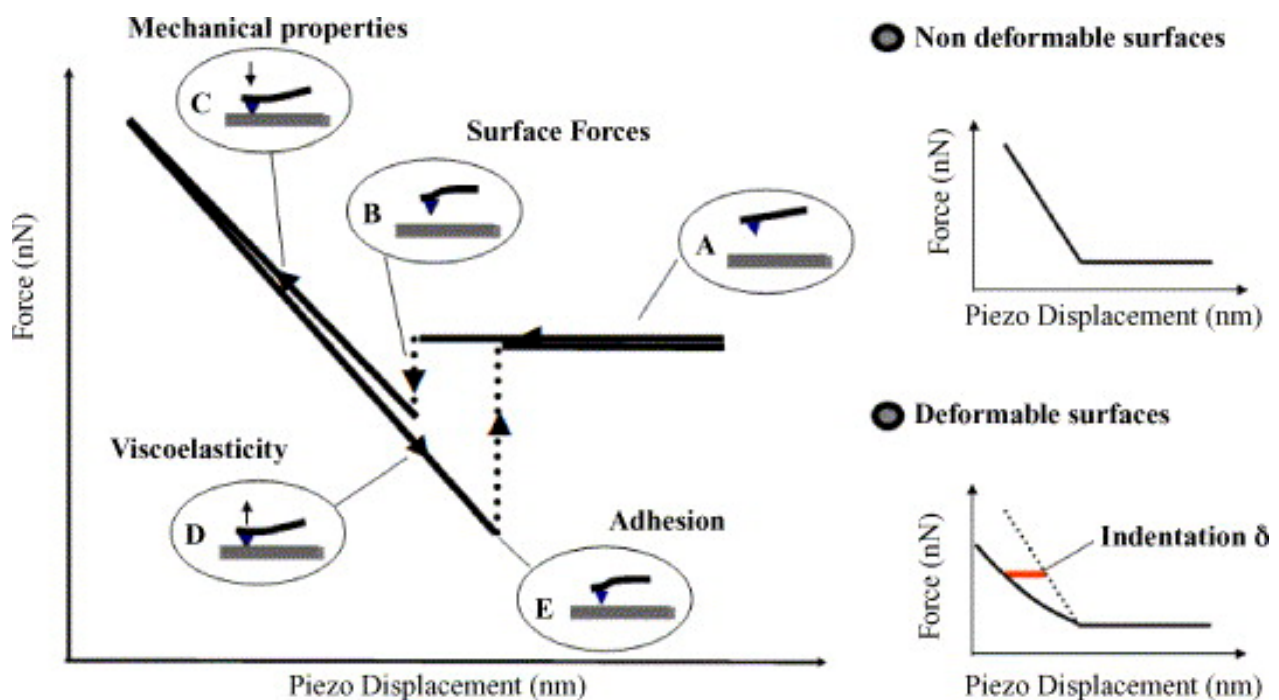


Figure 2. Representation of a typical force–distance curve. Reprinted with permission from [41].

#### 2.4. Scanning Modes

An essential aspect of AFM is its versatility in operating under different scanning modes, as mentioned earlier, each offering unique advantages and limitations. The most utilized scanning mode in AFM is contact mode. In contact mode, the cantilever makes direct contact with the sample surface, and the deflection of the cantilever is monitored as the probe scans across the surface. Contact mode excels at high-resolution imaging of surfaces with significant topographical contrast. However, it can potentially damage the sample surface and has limited sensitivity to other surface properties beyond topography, such as elastic modulus, surface roughness, and topography. Another popular scanning mode in AFM is tapping mode, also known as intermittent contact mode. In tapping mode, the cantilever vibrates at its resonant frequency, periodically contacting the sample surface. This minimizes harm to the sample surface and offers excellent sensitivity to non-topographical characteristics, such as material contrast, elasticity, and stiffness mapping, making it suitable for imaging delicate or soft samples. Nevertheless, tapping mode may compromise spatial resolution and can be more operationally intricate compared to contact mode. Another scanning mode employed in AFM is non-contact mode [43]. In this mode, the cantilever remains at a fixed distance from the sample surface, with the tip interacting with the surface through Van der Waals forces, and exhibits high sensitivity to surface forces, making it appropriate for imaging of fragile or easily affected samples. However, it possesses limited lateral resolution and can be influenced by environmental factors like temperature and humidity. The selection of a scanning mode relies on factors such as the type of sample, resolution requirements, and desired information content.

#### 2.5. Functionalization of AFM Tips

In the realm of life sciences or biomedical research, AFM tips are often tailored with specific chemical groups or molecules to enable the measurement of weak forces, including magnetic, adhesive, Van der Waals, electrostatic, and hydration forces, between the tip and the surface molecules. This is achieved through tip functionalization [44], which plays a critical role in enhancing the capabilities of AFM. A frequently used approach for functionalizing AFM tips [45] is through the nonspecific adsorption of probe molecules. This method is effective and uncomplicated; however, it is crucial to consider that the bonding strength of adsorption may not always exceed the specific interaction between the ligand attached to the tip and the target molecules on the surface. Moreover, directly immobilizing biomolecules onto an inorganic support can result in denaturation, degradation, and compression during the scanning process. To overcome these challenges, covalent bonding is employed to attach the probe to the tip, for which linear poly (ethylene glycol) (PEG) chains are often used. PEG provides benefits such as chemical and physical stability, enabling the probe molecule to reorient itself quickly and freely when the AFM tip interacts with the surface. This ensures that a single molecule on the tip can effectively identify its corresponding counterpart on the target surface. Various functionalization techniques can be employed by taking into account the specific molecules involved and the experimental requirements [46]. Daza et al. [47] explored the use of the activated vapor silanization (AVS) process to functionalize AFM cantilevers and tips. Thin films with specific desired functionalities were deposited onto silicon nitride chips, and their existence and performance were confirmed by assessing changes in the resonance frequency of the cantilever. To gain further insights into these films, fluorescein-derived molecules were covalently tethered to the amine-reactive groups present on the surface. As a result, the functionalized tips displayed resilient capabilities, withstanding repeated interactions with a model graphite substrate even under demanding conditions, while exhibiting no noticeable adverse effects. Additionally, the covalent attachment of a molecule to the tip permits the manipulation of the substrate–tip interaction. Another study by Girish et al. [48] showcased the successful functionalization of AFM tips using folic acid (FA) for the imaging of folate receptors (FRs) in oral cancer cell lines. This functionalization technique enables well-resolved phase images of FRs (Figure 3), offering insights into their distribution and characteristics.

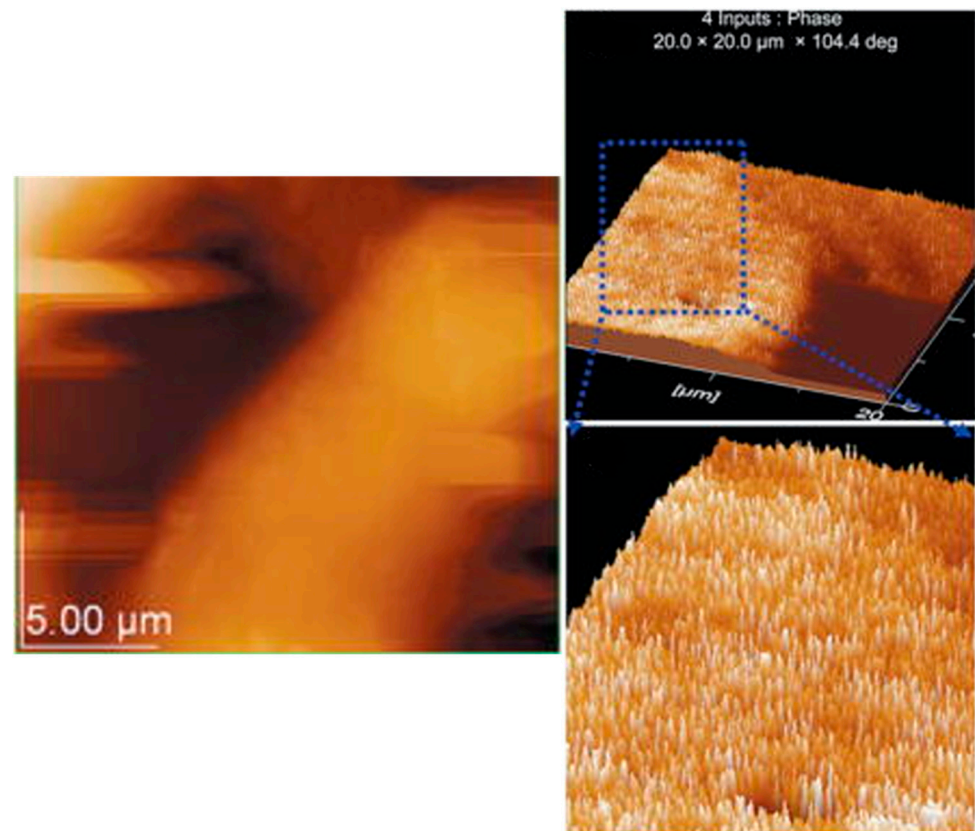


**Figure 3.** Topographic image and phase image of L929 cells, respectively, using an FA-functionalized tip. Density of receptors. *Applied Physics Letters*, 2009, 95(22): p. 223703. Reprinted with permission from [48].

## 2.6. Investigating Mechanical Properties of Biological Materials

AFM has emerged as a powerful and versatile tool for investigating the mechanical properties of biological materials at the nano scale. It allows one to probe and manipulate biological samples, providing valuable insights into their stiffness, elasticity, adhesion, and topography. Before determining mechanical properties, high-resolution imaging and surface topography of the biological sample should be obtained using AFM in contact mode or tapping mode. This step allows the visualization and selection of appropriate regions of interest for subsequent mechanical measurements, ensuring that the chosen areas are representative of the sample's properties. The force–distance curve is the primary technique used to determine mechanical properties using AFM. In this technique, the AFM tip is brought into contact with the sample surface, and a small indentation force is applied. The deflection of the cantilever is measured as a function of the piezo displacement, resulting in a force–distance curve. This curve provides information about the sample's response to applied forces and allows for the calculation of various mechanical properties.

### 2.6.1. Elasticity and Young's Modulus

From the force–distance curve [49], one can determine the elasticity or Young's modulus of the biological sample. Young's modulus is a key parameter for characterizing the mechanical properties of samples. It represents the stiffness, rigidity, or compliance of the material and can provide insights into intermolecular interactions. AFM nanoindentation is one of the most powerful techniques for the determination of Young's modulus. The main idea is to indent the sample surface with the AFM tip and to measure the applied load at each indentation depth. The cantilever base or the sample is moved vertically by a piezoelectric actuator (Z-axis), causing the tip–sample gap to decrease until contact occurs, and the cantilever tip experiences a repulsive force, deflecting while indenting the sample

of interest. Force–distance curves are typically composed of a baseline, contact between the tip and the surface, loading of the tip and indentation into the sample, the jump to contact point where the direction of the Z motion is reversed, adhesion where the tip is bound to the sample surface beyond the point of contact as the tip–sample contact is being separated, and finally, the return to zero interaction force, as shown in Figures 2 and 4. During the analysis of the force–indentation curves, the fitted function is assumed to take the form of the power law  $y = a \cdot x^b$ , where the value of  $b$  depends on the assumed shape of the intended AFM tip. The final Young’s modulus is calculated considering all values obtained from a whole set of force–indentation curves. The resulting distribution [50] is fitted with the Gaussian function. In force–distance curves, a steeper slope indicates a higher Young’s modulus, suggesting a more rigid or resistant region.

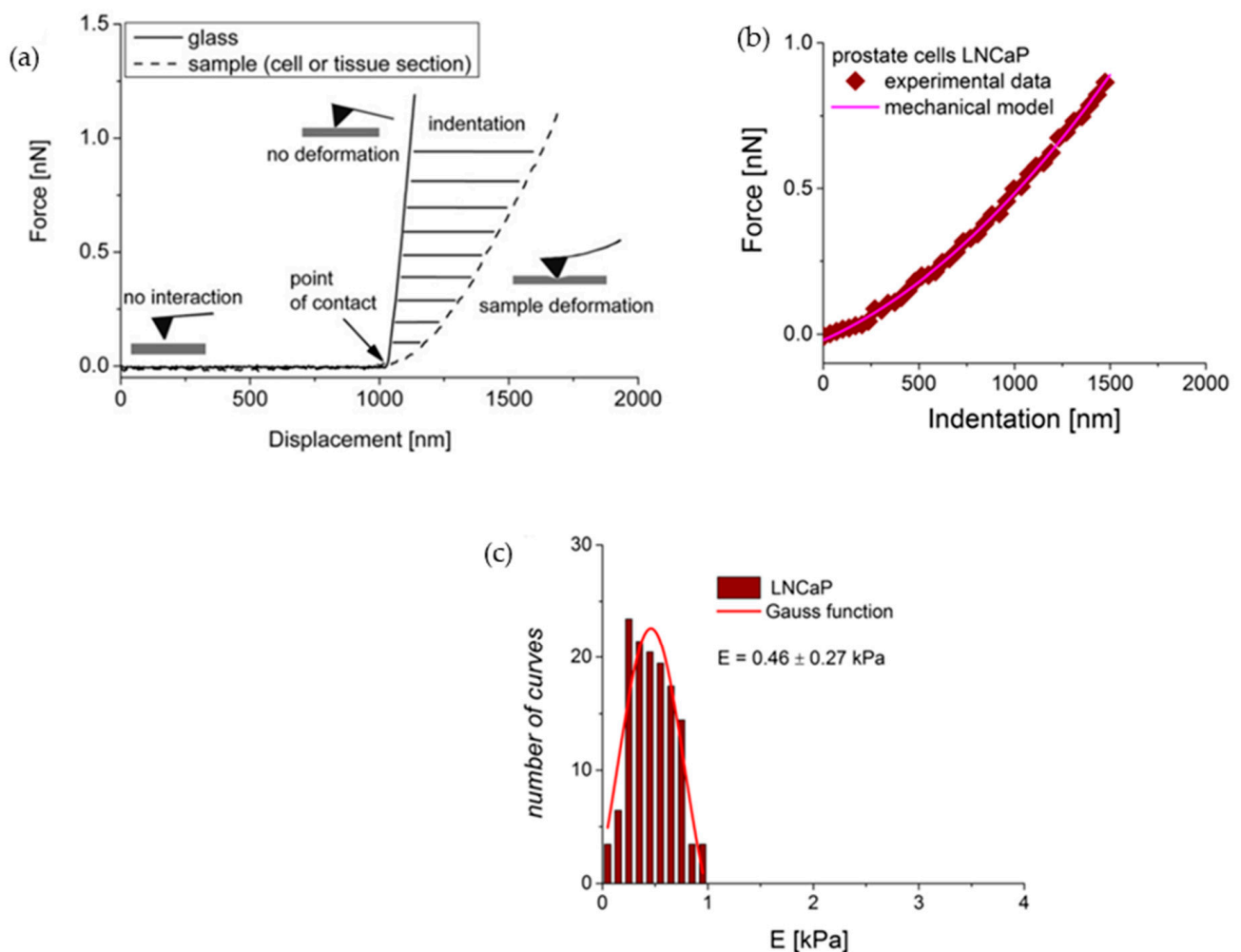


**Figure 4.** (a) The force–displacement curves measured for glass and a cell. Reprinted with permission from [49]. (b) The force–indentation curve fitted with the Hertz model. (c) Determination of Young’s modulus from the Gaussian function fit. Reprinted with permission from [50].

### 2.6.2. Adhesion Force

AFM force–distance curves provide valuable information about the adhesion properties between the AFM tip and the sample surface. By analyzing these curves, as shown in Figure 2, one can gain insights into the interactions and forces involved at the nanoscale level. The adhesion property is typically characterized by the adhesion force, which represents the force required to separate the AFM tip from the sample surface after contact. It is measured as a negative force value on the force–distance curve when the tip is being retracted. The magnitude of the adhesion force indicates the strength of the interaction

between the tip and the sample. In addition to the adhesion force, other parameters can be derived from the force–distance curve to assess the adhesion properties. These include the pull-off distance, which is the distance at which the tip completely detaches from the surface, and the adhesion energy, which represents the energy required to break the adhesive bonds between the tip and the surface. The shape and characteristics of the force–distance curve can provide further information about the adhesion properties. For example, a steep and abrupt increase in force during the approach phase, followed by a sudden drop during retraction, indicates strong adhesion between the tip and the sample. On the other hand, a gradual increase and decrease in force suggests weaker adhesion. By analyzing the adhesion properties obtained from AFM force–distance curves, one can gain insights into various phenomena and processes. This includes studying the adhesion between biomolecules, assessing surface properties and coatings, investigating the strength of molecular interactions, and understanding the adhesion mechanisms in biological systems.

Thus, AFM has revolutionized the characterization of mechanical properties of biological materials at the nano scale. Advancements in AFM technology continue to enhance our understanding of the mechanical properties of biological materials, contributing to various fields, such as biomaterials, tissue engineering, and biomechanics.

### 2.7. Recent Advancement in AFM

Significant variations in the measured properties of the same sample are often observed, which can be attributed to two primary sources: inherent biological diversity, and experimental inaccuracies. Experimental inaccuracies can stem from deviations in instrument performance and discrepancies in data gathering and analysis protocols. To counteract and diminish these errors, it is essential to undertake a comprehensive normalization endeavor spanning across multiple laboratories, instruments, and operators. This collaborative approach is vital for overcoming the inherent limitations associated with single-laboratory studies. Schillers et al. [51] introduced SNAP, a standardized nanomechanical AFM procedure that enhances the accuracy and reproducibility of mechanical measurements. It reduces variability in elastic modulus measurements for soft samples and living cells caused by technical factors and ensures precise calibration of the AFM optical lever system, independent of the instrument, laboratory, or operator. It addresses errors by accurately calculating deflection sensitivity (Figure 4) based on spring constants determined using a vibrometer. Wang [52] developed a practical transition model to explain complex ricin–aptamer interactions. It combines the Bell–Evans model and Markov-type transition matrices, providing detailed information about molecular structures, unbinding forces, and activation energies. This approach can be applied to study other single-molecule interactions with multiple reaction pathways. In addition, the authors proposed a method [53] that enables the investigation of binding conformations and affinities of biomolecules. The combination of AFM techniques and molecular simulations enables a novel approach for detecting and studying the mechanisms of aptamers. Adams et al. [54] achieved high-speed AFM imaging (HS-AFM) [55] in air by using SU-8 polymer cantilevers. These polymer-based cantilevers mimic the damping of liquid environments and provide an imaging-in-air detection bandwidth 19 times faster than conventional cantilevers with similar properties. Puppulin et al. [56] conducted a study for recognizing specific target molecules on mica substrates and lipid membranes. They focused on the MET receptor and used the macrocyclic peptide aMD4 to functionalize the HS-AFM tip. The imaging results revealed the selective interaction between the aMD4-conjugated tip and the hMET receptors, leading to enhanced phase delay in the cantilever’s oscillation. By using aMD4, they were able to discriminate between human MET and the murine homologue. Yang et al. [57] introduced an advanced platform for nanoscale analysis called spectral-spatially encoded array AFM (SEA-AFM) (Figure 5). Unlike conventional methods, it utilizes alternative readout techniques, such as piezoelectric sensors and high-resolution optical detection, to enable simultaneous and independent addressing of multiple cantilevers. Thus, this method successfully tackles interferences while preserving remarkable sensitivity and expandability, thereby present-

ing a formidable instrument for thorough nanoscale analysis with enhanced efficacy and versatility.

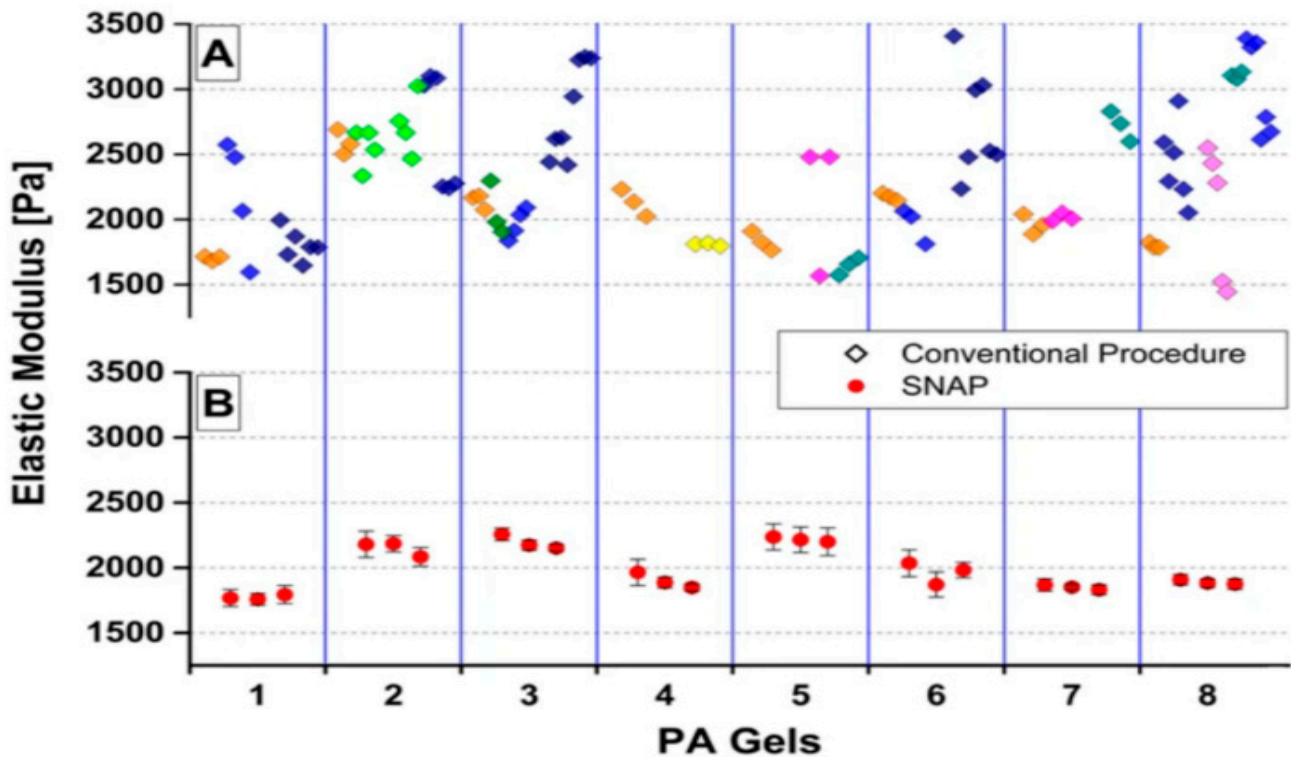


**Figure 5.** Elastic modulus of gels from different labs measured using (A) a conventional procedure and (B) using SNAP. Reprinted with permission from [51].

Park et al. [58] developed a novel technique called DP-pAFM (Figures 6 and 7) for high-resolution morphological and optical analysis of samples, which offers improved image contrast and sensitivity while avoiding excessive power, thereby minimizing the risk of damage to the sample or the cantilever tip. Two identical lasers generate separate beams with a controlled time delay, which are combined using mirrors and a beam splitter, coupled into a single-mode fiber, and obliquely illuminated onto the target sample through a focusing system. The first laser heats the area under the cantilever tip, followed by the second laser after a short delay. This induces unique cantilever oscillations, allowing for the mapping of optical structures in small-molecule semiconductor films.

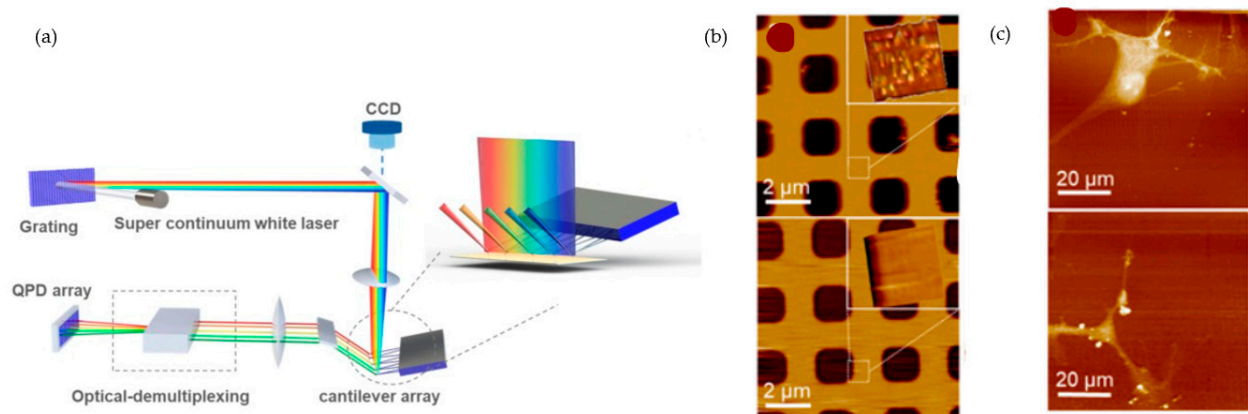


**Figure 6.** (a) SEA-AFM system. (b) Calibration grid of 3  $\mu\text{m}$ . (c) AFM image of fixed neural progenitor cells. Reprinted with permission from [57].

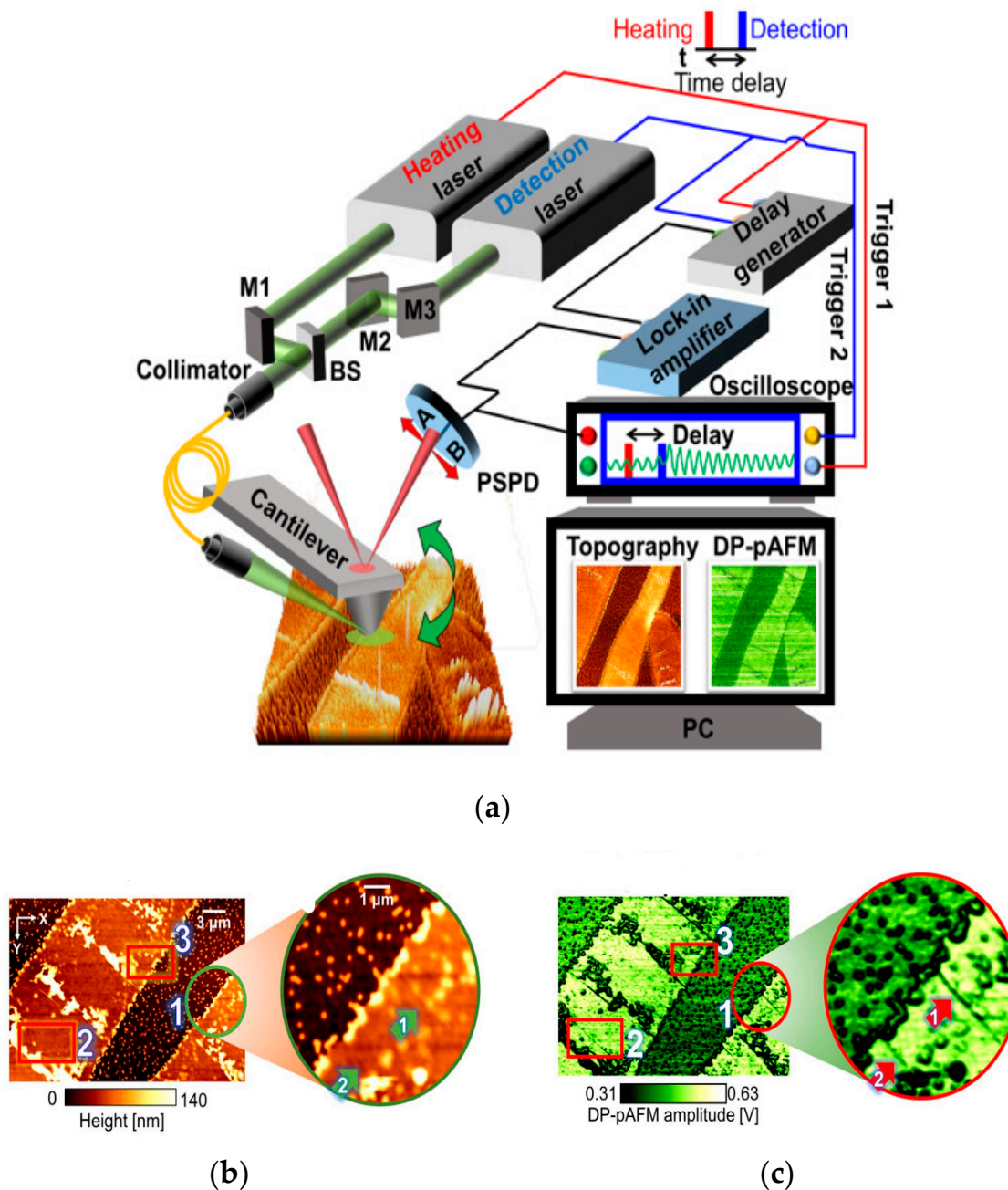


**Figure 7.** (a) Schematic diagram of DP-pAFM. (b,c) Topographic images of SP- and DP-pAFM, respectively. Figure (a,b,c) reprinted with permission from [58].

Cheng et al. [59] introduced an algorithm called network-based automatic clustering algorithm (NASA) to address the challenge of automatically specifying unbinding forces to binding sites in single-molecule data. It extracts unbinding forces, constructs a network representing their relationships, and detects community structures corresponding to binding sites. They applied NASA to decode the interaction between heparan sulfate (HS) and antithrombin (AT) on different endothelial cell surfaces as a model system, successfully detecting peaks, calculating unbinding forces, and identifying three force clusters that corresponded to different binding sites. NASA shows potential for analyzing other AFM-based measurements, such as antibody–antigen and DNA–protein interactions, characterized by “saw-tooth” force–distance curves with force-induced unbinding events.

### 3. Applications of AFM in the Study of Biomolecules

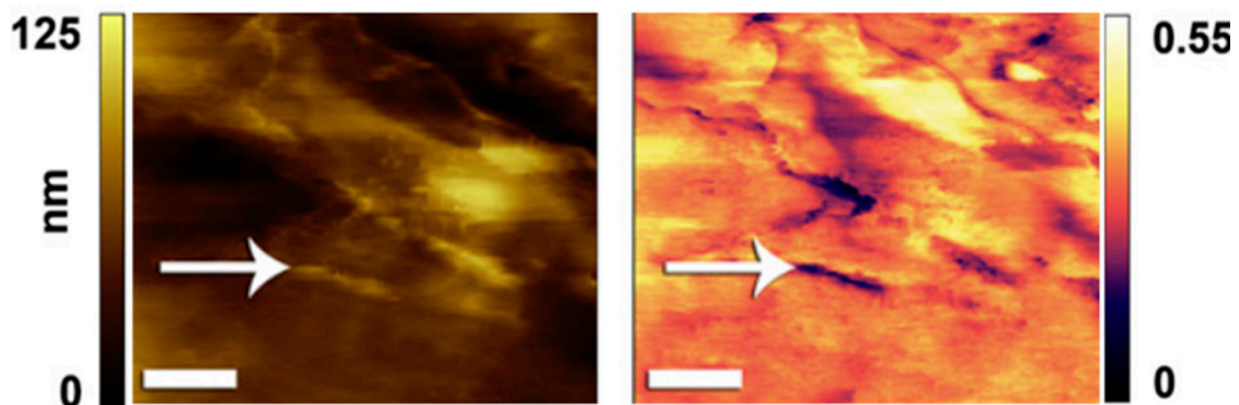
AFM enables the visualization of biomolecules in three dimensions, providing valuable insights into their shape and structure at the nano scale. It operates in diverse environments, making it suitable for studying biological systems. It plays a crucial role in investigating biomolecular interactions, including protein–protein, lipid–protein, and DNA–protein interactions. It allows direct, label-free measurements of molecular forces and interaction energies, facilitating the study of structural and mechanical properties. In this section, we explore the application of AFM as a tool for studying transport phenomena in biological interactions.

#### 3.1. Protein

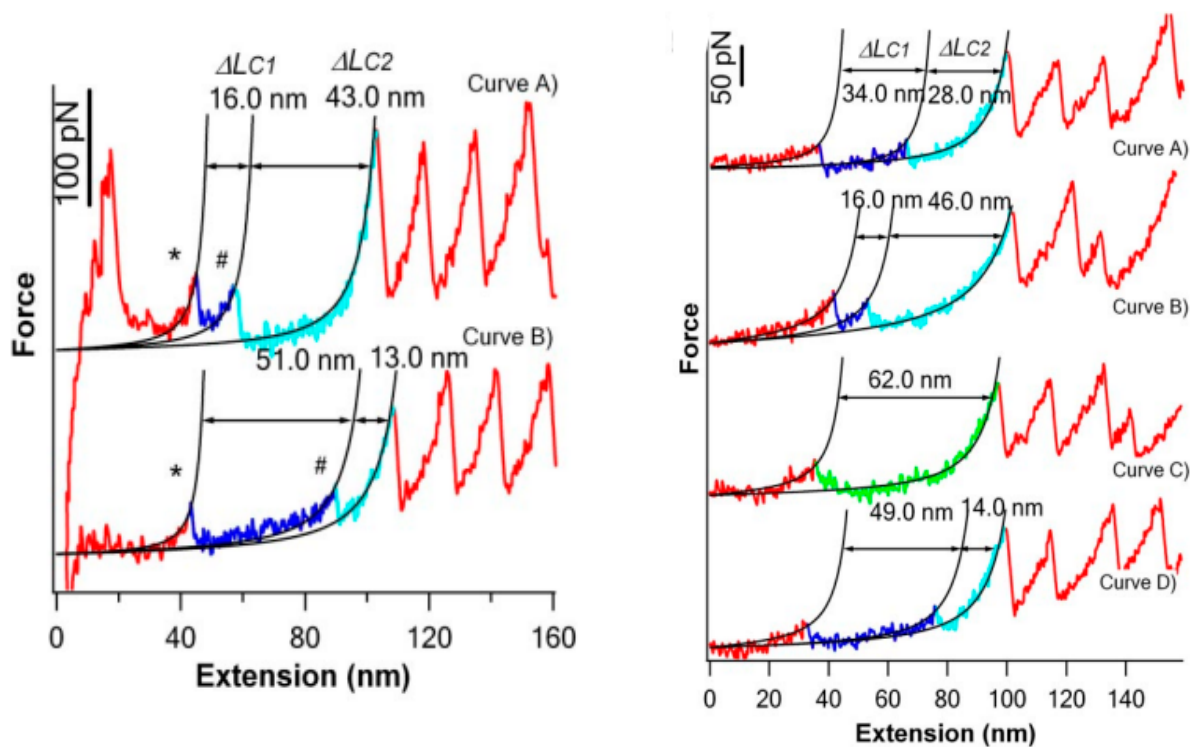
Proteins play a vital role in biological systems, participating in essential cellular processes such as protein synthesis, signal transduction, and enzymatic reactions. They are also implicated in the development of various diseases, including neurodegenerative disorders like Parkinson’s and Alzheimer’s, as well as localized conditions such as type 2 diabetes and cataracts. Understanding protein aggregation is crucial in clinical settings for comprehending disease pathology and developing diagnostics and therapies. One example of protein aggregation is pseudoexfoliation syndrome (PEX), a disorder characterized by extracellular matrix protein aggregation that obstructs the eye’s aqueous outflow, posing a significant risk of glaucoma. Creasey et al. [60] utilized AFM-based antibody recognition imaging (Figure 8a) to investigate the molecular nature of PEX aggregates on human lens capsules. Their findings revealed an association between lysyl oxidase-like 1 (LOXL1) and an increased susceptibility to the syndrome. Another notable example is Alzheimer’s disease, which is characterized by the self-assembly and accumulation of fibrillar amyloid- $\beta$  (A $\beta$ ) peptides in the brain. Biophysical studies, including AFM, have significantly advanced our understanding of the mechanisms underlying amyloid formation and its role in the pathogenesis of Alzheimer’s.

AFM plays a crucial role in studying protein folding and unfolding processes, which are fundamental to cellular function. Proteins transition from an unfolded state to well-defined three-dimensional structures, unique to each protein, for their biological activity. AFM enables direct visualization of the topographic structures of individual proteins and provides mechanical insights into their unfolding dynamics. Protein misfolding can lead to the formation of aggregated protofibrils, contributing to various diseases, such as Alzheimer’s, prion diseases, cystic fibrosis, and amyotrophic lateral sclerosis. AFM studies on protein folding have focused on proteins with tandem repeats of similar modules, such as tenascin, spectrin, and titin, which exhibit mechanical strength that is essential for their physiological functions. Best et al. [61] aimed to investigate the resistance of proteins to force and discovered that proteins that are not specifically designed for tensile strength may not exhibit the same resistance to force as those that are. They also observed that proteins with similar unfolding rates in solution may exhibit different unfolding properties under force, emphasizing the importance of considering protein-specific characteristics when studying their response to mechanical forces using AFM. Kawakami and Smith [62] introduced a novel force-ramp modification that enables precise control of multiple unfolding events in a multi-modular protein. This advancement utilizes software-based digital force feedback control to maintain a constant force-loading rate, regardless of the length of the soft elastic linkage or the number of unfolded polypeptide domains. By applying this technique, one can observe distinct pathways of unfolding in a controlled manner. Peng and Li. [63] conducted an experimental study that provided empirical evidence for the kinetic partitioning mechanism involved in the mechanical unfolding of T4 lysozyme—a compact protein composed of two subdomains. By subjecting T4 lysozyme to applied stretching forces from its N and C termini, they observed multiple distinct pathways of unfolding (Figure 8b,c). The majority of T4 lysozyme molecules exhibited an all-or-none unfolding behavior, surpassing a dominant kinetic barrier. However, a minority fraction of T4 lysozyme molecules followed a three-state unfolding pathway involving intermediate

states. Notably, these three-state unfolding pathways displayed variability and diversity, deviating from well-defined routes. These findings provide direct evidence for the presence of kinetic partitioning in the mechanical unfolding pathways of T4 lysozyme. Moreover, the complex unfolding behaviors observed highlight the stochastic nature of kinetic barrier rupture during mechanical unfolding processes. In a study by Mahmood, Moheimani, and Bhikkaji [64], the effectiveness of integrating genetic manipulation with the AFM technique was investigated as a robust method to study the responses of proteins to forces within living cells. The findings underscore the potential of this approach for unraveling the intricate mechanisms underlying protein mechanics in a cellular context. Thus, AFM studies have significantly contributed to our understanding of proteins' aggregation, folding, and unfolding processes. They shed light on the structural and mechanical properties of proteins, offering insights into their biological functions and their roles in disease development.



(a)



(b)

(c)

**Figure 8.** (a) AFM images of a lens capsule from a PEX patient acquired using an anti-LOXL1-antibody-functionalized tip, from an area near the center of the capsule. Reprinted with permission

from [60]. (b) Typical force–extension curves of cysteine-free pseudo wild-type T4 lysozyme (T4L\*) showing three-state unfolding behaviors. (#-second unfolding force peaks) (c) A series of force–extension curves of the same T4L\* measured during repeated stretching–relaxation experiments. Reprinted with permission from [63].

### 3.2. Nucleic Acids

The direct imaging of nucleic acids [65] in aqueous solutions has long been a challenging task, primarily because of the relatively weak interactions between nucleic acids and substrates. However, advancements in substrate modifications and detection methods have improved the quality and resolution of nucleic acid imaging. Zhu et al. [66] provided a method for studying DNA methylation that cannot be detected using conventional DNA probes. They used an antibody-tethered AFM cantilever to measure the distances between 5-methylcytidine bases in DNA strands, with a resolution of 4 Å. By binding to two 5-methylcytidine bases, the cantilever retraction produced a unique rupture signature reflecting the spacing between the tagged bases. Shim et al. [67] developed a force mapping method to directly quantify low-abundance DNA containing methyl-CpG at a specific site. Their approach utilized methyl-CpG-binding (MBD) proteins to distinguish methylation states. The MBD protein was positioned on the probe opposite the target DNA site of interest. If the target site was methylated, the MBD protein would identify the methylated CpG, while it would disregard the site if it was not methylated. This method allowed for the detection of specific methylation patterns without the need for chemical treatment or amplification of the target DNA. Strobl et al. [68] investigated the factors influencing nucleic acid condensation and release in individual parvovirus particles. A single virus particle was attached to a cantilever and exposed to various physicochemical conditions, where the pH and salt concentration were manipulated to induce the condensation or release of nucleic acids. The study revealed that parvovirus particles are highly responsive to changes in physicochemical conditions for nucleic acid condensation and release.

### 3.3. Polysaccharides

The application of AFM in the study of polysaccharides [69] is not as extensive as it is for other biomolecules, despite the crucial biological roles that they play. Nevertheless, there have been several AFM investigations that have aimed to unravel the structural characteristics of polysaccharides found in bacteria, plants, and fungi, as well as densely glycosylated peptides and proteoglycans. Furthermore, AFM proves valuable in exploring the molecular interactions between polysaccharides and other biomolecules, such as proteins and lipids. In addition to these efforts, recent advancements in AFM techniques offer opportunities to delve deeper into the characterization and functional analysis of polysaccharides, providing a promising avenue for future research in this field. An example of interest in this field is the investigation of heparan sulfate (HS), a linear polysaccharide found in all animal cell plasma membranes. Guo et al. [70] investigated the interaction between heparan sulfate (HS) and antithrombin (AT) on the surface of a single endothelial cell under near-physiological conditions to understand the role of critical sulfates responsible for AT binding. The specific interaction between HS and a protein ligand is primarily determined by the sulfation patterns on the HS chain. The research revealed that AT interacts with endothelial HS through multiple binding sites, and the presence of N-, 2-O-, and/or 6-O-sulfates on HS is essential for this interaction.

### 3.4. Peptide

Peptides are short chains of amino acids that can have a wide range of functions in biological systems, including signaling molecules, neurotransmitters, cell regulation and homeostasis, etc. Li et al. [71] conducted a study focusing on peptide-assembled hydrogels, investigating the morphology and mechanical properties of individual nanofibrils during the gelation and degradation processes of these hydrogels. With the help of topographic imaging, they were able to observe distinct assembly behaviors of peptide-formed nanofibrils throughout the gelation and degradation stages, revealing a correlation between these behaviors and changes in nanofibrillar mechanics. Gaspar et al. [72] conducted a study investigating the impact of a peptide called APN-1 on the mechanical characteristics of cancer cells. Their findings revealed that APN-1 can induce alterations in the mechanical properties of cancer cells, resulting in cell death and suppressed tumor growth. Specifically, APN-1 was observed to enhance the stiffness of cancer cells and disrupt their cytoskeleton—a network of protein fibers responsible for cellular structural support. These changes in mechanical properties were associated with increased cell death and diminished tumor growth. These findings suggest the potential of APN-1 as an antitumor agent, with its effects on cellular biomechanics playing a crucial role in its therapeutic activity.

### 3.5. Enzymes

Enzymes help in speeding up chemical reactions in physiological processes such as digestion, metabolism, and DNA replication. Enzymes have been extensively studied due to their significance and diverse applications. Zhang et al. [73] investigated the enzymatic hydrolysis of pretreated biomass and observed real-time changes in the cellulose structure of plant cell walls during enzymatic hydrolysis (Figure 9a,b). The enzymes' action depended on the size and width of the cracks in the cellulose. Smaller cracks led to progressive degradation, while larger cracks caused the peeling of glycan chains. The combination of CBH I and  $\beta$ -G enzymes effectively hydrolyzed the biomass, emphasizing the role of crack size in the depolymerization and peeling of cellulose microfibrils. Cellulolytic enzymes, such as CBM3a, play a crucial role in binding specifically to crystalline cellulose. Zhang et al. [74] utilized CBM3a-functionalized gold nanoparticles (GNPs) to monitor the binding activity of CBM3a to poplar cell-wall cellulose. The GNPs-CBM3a complexes showed specific binding to the cellulose surface, aligning with the cellulose fibril axis. This work advances the comprehension of biomass–enzyme interactions and facilitates the development of efficient cellulolytic enzymes for biofuel production. In their research, Zhang and Wang et al. [75] investigated the affinity interactions between the carbohydrate-binding module (CBM) and plant cell-wall cellulose at the single-molecule level. They used AFM tips functionalized with CBM3a and CBM2a to determine the binding efficiencies of CBMs to cellulose. Recognition imaging (Figure 9c) revealed that CBM3a exhibited slightly higher binding efficiency and affinity than CBM2a on both natural and extracted cellulose surfaces. Moreover, both CBMs showed higher affinities towards natural cell-wall cellulose microfibrils compared to extracted single cellulose microfibrils. This study provides valuable insights into the binding properties of CBMs to cellulose, highlighting the differences between CBM3a and CBM2a and their interactions with cellulose surfaces. They [76] also further examined the CBM–cellulose binding process on extracted crystalline cellulose. CBM3a molecules were utilized for both functionalizing the AFM tip and binding as free CBM molecules. The in situ AFM imaging revealed the efficient and regular binding of CBM molecules to cellulose, particularly within the initial 60–120 min. This research significantly contributes to in-depth understanding of the binding mechanism between CBM and crystalline cellulose at the single-molecule level.

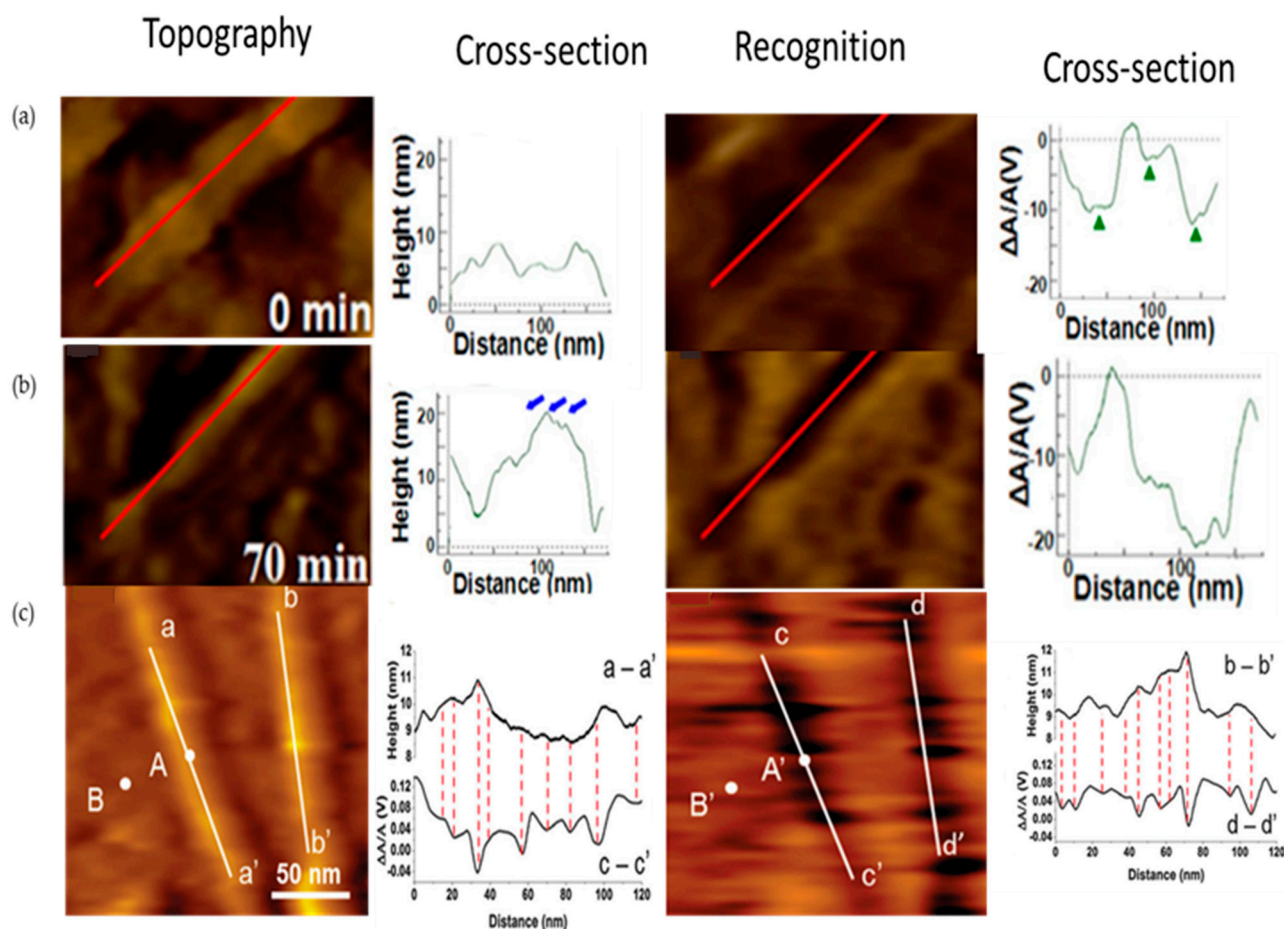


**Figure 9.** (a,b) Topography, recognition images, and cross-sectional analysis of pretreated poplar cellulose incubated with EG at 0 and 70 min, respectively. Reprinted with permission from [73]. (c) Extracted single cellulose microfibrils. Reprinted with permission from [75].

#### 4. AFM for Studying Transport Phenomena in Biological Interactions

Recent advancements in scanning probe microscopy techniques have expanded the application of force microscopy in biology, providing simultaneous and specific information about biological interactions. One area of focus is the study of transport phenomena in biological interactions, which can be investigated by assessing molecule interaction dynamics. AFM is particularly useful in studying protein–ligand interactions, as it can measure bond rupture forces, revealing information about affinity and kinetics. Furthermore, AFM enables the visualization of cell surfaces and their interactions with substrates, offering insights into important cellular processes such as adhesion, migration, and differentiation. Endothelial cells, which act as a barrier between blood and underlying tissues, are particularly intriguing for AFM investigations. Kolodziejczyk et al. [77] conducted a study on endothelial cells (EA.hy926) exposed to silver nanoparticles. They discovered that the elasticity of the cells decreased with higher concentrations of silver nanoparticles, potentially due to cytoskeleton reorganization and reinforcement of the cell cortex caused by the presence of nanoparticles. Additionally, agglomerates of silver nanoparticles were observed on the cell membrane and inside the cells. These findings suggest that force spectroscopy can serve as a bio-indicator of the physiological state of endothelial cells when exposed to nanoparticles. In another study, Dong and Sahin [78] investigated bond lifetimes, observing notable increases in molecular interaction forces with lifetimes of approximately 5  $\mu$ s. This nanomechanical interface provides opportunities for studying shortlived molecular processes and advancing biological imaging, single-molecule manipulation, and assembly technologies. By utilizing AFM, one can gain valuable insights into the dynamic nature

of biological interactions and contribute to the development of various fields within the biological sciences.

#### 4.1. Unraveling the Mechanics of Antigen–Antibody Interactions

Antigen–antibody interactions [79,80], which involve the binding of an antibody molecule to a specific antigen molecule (typically a protein or carbohydrate on the surface of a pathogen or target molecule), can be studied using AFM. This technique allows for the measurement of interaction strengths and bond breaking, providing valuable information about the strength and specificity of the interaction. Hinterdorfer et al. [81] investigated recognition events between antibodies and antigens, as well as the localization of antigenic sites. They observed unique force signals with an unbinding force of  $244 \pm 22$  pN for single antibody–antigen recognition events. The unbinding forces were found to result from the dissociation of individual Fab fragments from a human serum albumin molecule. The study revealed that the two Fab fragments of the antibody demonstrated independent and equiprobable binding, facilitated by a flexible linkage that allowed for a 6 nm range of binding and a high binding probability of 0.5 within encounter times of 60 ms. In a study by Berquand et al. [82], the forces involved in antigen binding were examined by studying individual Fv fragments of anti-lysozyme antibodies. The force–distance curves exhibited the rupture of a single antibody–antigen pair. The injection of free lysozyme led to a significant decrease in adhesion probability, confirming the specificity of the antibody–antigen interaction. By recording force–distance curves at different loading rates, the study revealed two distinct linear regimes with increasing slopes, indicating the presence of multiple energy barriers in the interaction dynamics. Kienberger et al. [83] focused on investigating the strength of molecular binding between antibodies and their corresponding antigenic sites. They examined the binding of anti-Sendai antibodies to Sendai epitopes fused into bacteriorhodopsin molecules. By studying bacteriorhodopsin’s unfolding, the study observed distinct intramolecular force patterns, allowing for clear differentiation between wild-type and Sendai bacteriorhodopsin molecules based on their length distributions. The unbinding force between the antibody and antigen was significantly lower than the force required to extract and unfold the epitope-containing helix pair from the membrane, indicating that the intermolecular unbinding forces were weaker than the intramolecular unfolding forces responsible for maintaining the native protein conformation. Chen et al. [84] conducted a study on the interactions between the HIV-1 envelope protein gp120 and its receptors, sCD4 and CD4. They examined the binding and dissociation forces involved in the gp120–sCD4 and gp120–CD4 antigen–antibody interactions. The results showed that the binding forces of gp120–sCD4 were stronger compared to those of gp120–CD4 antigen–antibody interactions. Additionally, they investigated the impact of glycosylation on the gp120–sCD4 interaction and found that the presence of carbohydrates weakened the interaction. Thus, AFM proves to be a powerful tool for studying antigen–antibody interactions, providing insights into their structure, binding mechanisms, and specificity. This technique enables the investigation of bond rupture forces, localization of antigenic sites, and characterization of molecular binding strengths, contributing to a better understanding of these interactions in various biological contexts.

#### 4.2. Aptamers: Versatile Tools for Molecular Probing

Aptamers [85], as small and chemically stable biomolecules, offer high affinity and specificity in binding to targets, serving as versatile alternatives to antibodies for molecular recognition. Wang and Yadavalli [86] demonstrated the versatility of oligonucleotide aptamers as probes for imaging and spatially locating targets on surfaces. By coupling DNA aptamers with force recognition mapping, they successfully localized specific proteins at the single-molecule level and detected changes in binding due to environmental variations. Topographic images revealed distinct protein patterns on the surface, and the measured unbinding forces aligned with individual interactions between the DNA aptamer and protein. In a significant development related to aptamers, Junior et al. [87] devised a rapid

NS1 detection platform using a specific DNA aptamer and electrochemical techniques. The non-structural protein NS1 encoded by the dengue virus exhibits continuous secretion into the bloodstream by infected host cells. The aptamer-based sensor showed exceptional sensitivity across a wide dynamic range in both buffer and undiluted human serum, offering rapid response time, cost-effectiveness, and high selectivity against other dengue proteins. It effectively detected serotypes 1 and 4 within clinically relevant ranges for primary and secondary infections, paving the way for potential application in miniaturized devices and point-of-care settings. Leitner et al. [88] conducted an insightful investigation into the interaction between the DNA aptamer sgc8c, immobilized on an AFM tip, and its corresponding receptor, protein tyrosine kinase-7 (PTK7), present in the membrane of acute lymphoblastic leukemia cells (Jurkat T cells). The aptamer exhibited remarkable affinity and specificity for binding to PTK7. Through concurrent topography and recognition imaging experiments (TREC) employing AFM tips functionalized with sgc8c aptamers on immobilized Jurkat cells, they achieved label-free determination of PTK7 distribution under near-physiological conditions. In a related study by Poturnayová et al. [89], interactions between the DNA aptamer sgc8c and protein tyrosine kinase (PTK7) were investigated in the membranes of leukemia lymphoblastic (MOLT-4) and lymphocyte cell lines, as well as PTK7-negative U266 myeloid leukemia cells. They utilized the thickness shear-mode acoustics method, developing an extremely sensitive, label-free biosensor for detecting leukemia cells. The biosensor demonstrated an impressive limit of detection of  $195 \pm 20$  cells/mL.

These pioneering investigations shed light on the fascinating interplay between DNA aptamers, their target receptors, and their applications in label-free imaging and biosensing for leukemia cells. The use of aptamers in conjunction with advanced techniques and technologies holds promise for advancements in molecular recognition, diagnostics, and therapeutic applications.

#### 4.3. Understanding Interactions in Polymer Systems

Understanding the interactions in polymer systems is crucial for advancing various fields, including biofuel production. Lignocellulosic biomass, a promising renewable resource for biofuel production, consists of cellulose, hemicellulose, and lignin. However, the presence of lignin poses a significant challenge, as it inhibits the enzymatic conversion of cellulose into glucose. Specifically, lignin causes cellulase enzymes, responsible for breaking down cellulose, to bind irreversibly to it, deactivating the enzymes and reducing their overall activity. To gain a better understanding of the non-productive binding phenomenon [90] between lignin and cellulase enzymes, which hinders the enzymatic conversion of cellulose into glucose in lignocellulosic biomass used for biofuel production, Qin, Clarke, and Li [91] embarked on a study to investigate the interactive forces involved in this interaction. Their objective was to identify the underlying mechanisms and factors contributing to the reduced activity of cellulase in the presence of lignin. To conduct their investigation, they utilized specialized tips with specific moiety groups attached to them. These modified tips allowed them to examine the interaction forces between immobilized cellulase and different surface chemistries. Specifically, they compared hydrophobic tips with COOH- and OH-coated tips. The results of their study were intriguing. They found that the interaction forces between the hydrophobic tips and cellulase exhibited the highest adhesion, surpassing the adhesion forces from COOH- and OH-coated tips by 13% and 43%, respectively. These findings indicated that hydrophobic–hydrophobic interactions played a significant role in the non-productive binding of cellulase to lignin in this simplified enzymatic hydrolysis system. The implications of these findings are substantial. By uncovering the importance of hydrophobic interactions in the non-productive binding of cellulase to lignin, one can devise strategies to mitigate this interaction and improve the efficiency of enzymatic biofuel production processes. Developing methods to minimize the binding of cellulase to lignin will enhance the overall activity and effectiveness of the enzyme, leading to increased glucose yield and improved biofuel production. Understanding the intricate interactions within polymer systems, such as the interaction between

lignin and cellulase, opens up avenues for targeted modifications and advancements in biofuel production. By gaining insights into these fundamental processes, one can optimize enzymatic hydrolysis and overcome the challenges posed by lignin, bringing us closer to sustainable and economically viable biofuel production.

#### 4.4. Investigating Protein Interactions through AFM Manipulation

Protein–protein interactions [92,93] are fundamental to the normal functioning of biological systems, playing critical roles in a wide range of biological processes, including signaling, transport, and regulation. Assessing these interactions using AFM involves the manipulation of individual proteins or protein complexes to measure the forces required for separation. The microvascular endothelium, which forms a monolayer of cells along the inner surface of blood vessels, serves as a vital structural barrier between the bloodstream and surrounding tissues. Due to its significant role in tissue and organ homeostasis, the microvascular endothelium holds substantial diagnostic and therapeutic potential. Endothelial cells exhibit complex morphology and functionality depending on their location within the body, actively contributing to maintaining homeostasis. Liver sinusoidal endothelial cells (LSECs), characterized by fenestrae and sieve plates, represent the most permeable type of endothelium, providing insights into their physiological state. Recent advancements in AFM imaging techniques have facilitated successful visualization of both fixed and live LSECs [94]. In a notable study conducted by Bonanni et al. [95], the molecular interaction between the protein C551 and gold-immobilized AZ was meticulously examined using AFM. The proteins were strategically positioned on both the substrate and the AFM tip to facilitate their mutual interaction. AZ was immobilized on gold via specific residues, orienting the protein configuration in a manner that ensured that its hydrophobic patch, responsible for interaction with C551, faced away from the electrode surface and towards the AFM tip. This study highlighted the significance of protein–protein interactions in biological systems and underscored the potential of AFM in investigating these interactions. The regulation of gene expression heavily relies on DNA-binding proteins, which play critical roles across various organisms, from bacteria to mammalian cells. These proteins interact with DNA, and their significance extends to numerous essential biological processes, such as DNA replication, packaging, and repair. Interference in DNA–protein interactions is implicated in various diseases. Manipulating these interactions through chemical means enables control over gene expression, offering potential therapeutic interventions for numerous ailments. A study conducted by Sanchez, Humberto, et al. [96] focused on the interaction between human RAD54w protein and DNA. They investigated the dynamic interaction of RAD54 with the sample surface and its influence on protein mobility. They observed that the presence of ATP and AMP-PNP in the imaging buffer affected the protein's diffusion constant. Anomalous diffusion behavior was observed when the protein interacted with surrounding molecules, such as DNA. The study further revealed that RAD54 moved along DNA through diffusion, and protein translocation in a DNA-crowded environment increased the likelihood of hopping and facilitated transfer to different DNA locations. Despite the development of various techniques, the understanding of DNA–protein interactions remains incomplete. The initial step in such studies involves identifying and isolating DNA-interacting proteins. Advancements in AFM and related techniques continue to contribute valuable insights into the intricate mechanisms and dynamics of these interactions, leading to a deeper understanding of biological processes and potential therapeutic strategies.

#### 4.5. Carbohydrate Recognition in Biological Systems: Exploring Receptor Specificity

Carbohydrates play a pivotal role in the composition of the cell membrane and actively participate in diverse biological processes, including energy production, cellular adhesion, and glycosylation. Lectins, which are proteins that bind to specific sugars, play a critical role in recognizing glycoconjugates and exhibit a distinct affinity for their corresponding sugar components. Gaining insights into the molecular interactions between lectins and

carbohydrates is fundamental to understanding cellular interactions and exploring innovative bioanalytical applications. In a study conducted by Touhami et al. [97], the interaction between the lectin concanavalin A (Con A) and oligoglucose saccharides was investigated. Gold-coated substrates functionalized with Con A and hex saccharide molecules terminated with thiols were utilized. Analysis of force–retraction curves revealed that approximately half of the curves displayed unbinding forces of  $96 \pm 55$  pN, accompanied by elongation forces and rupture lengths ranging from 0 to 200 nm. These characteristics were absent in measurements conducted with mannose or a hydroxyl-terminated probe. The obtained results confirm that the measured unbinding forces arise from specific interactions between the lectin and carbohydrates. In another study by Zhang et al. [98], AFM recognition imaging was employed to examine structural changes in crystalline cellulose on the cell-wall surfaces of poplar, switchgrass, and corn stover. The effects of natural dilute sulfuric acid pretreatment and delignification were investigated. The results indicated that the coverage of crystalline cellulose on the cell-wall surface increased from 17–20% to 18–40% after dilute acid pretreatment at 135 °C, with variations based on the acid concentration (Figure 10a–c). After delignification, the coverage reached 40–70%. These findings highlight the efficacy of dilute acid pretreatment in enhancing the accessibility of cellulose on plants' cell-wall surfaces. Through these studies, a deeper understanding of the role of carbohydrates in biological processes and their interactions with proteins can be obtained, paving the way for advancements in bioanalytical techniques and applications. The molecular insights provided by AFM investigations contribute to the development of innovative approaches for studying and manipulating carbohydrate–protein interactions, which have significant implications in various fields, including drug discovery, biomaterial engineering, and diagnostics.

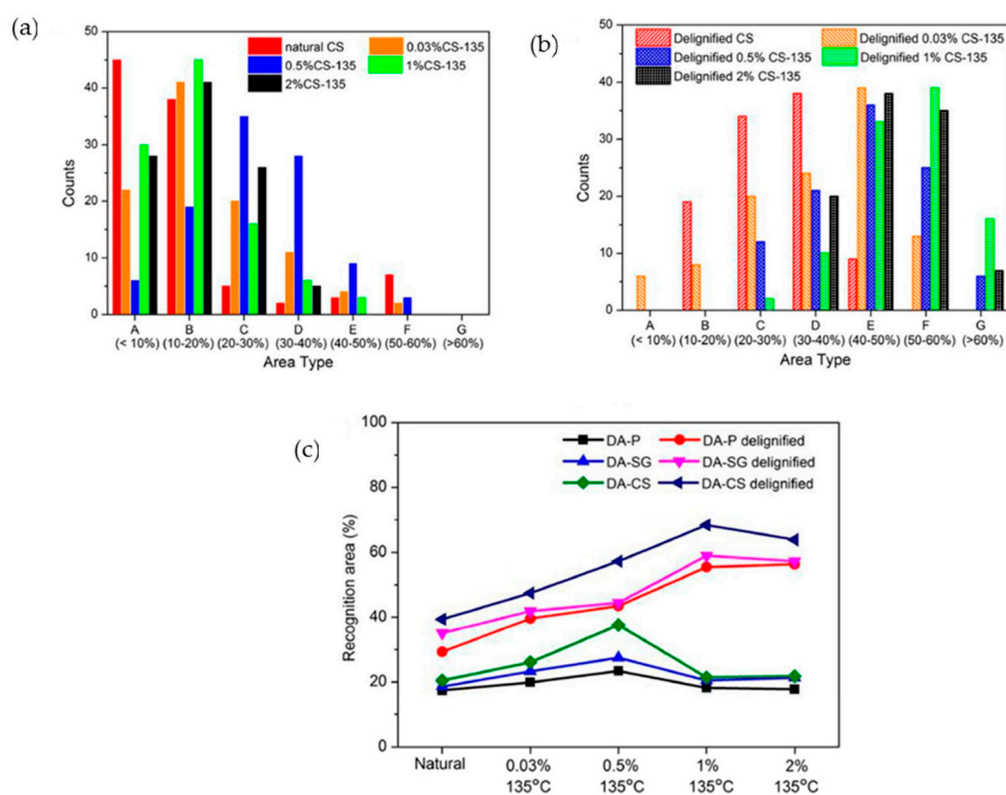


**Figure 10.** (a) Area type distributions of natural and dilute-acid-pretreated cell-wall surfaces of corn stover. (b) Area type distributions of delignified cell-wall surfaces of corn stover. (c) Recognition area percentage (RAP) summary of natural and pretreated poplar, switchgrass, and corn stover cell-wall surfaces. Reprinted with permission from [98].

## 5. Unveiling the Mechanical Properties of Cells

Cells are complex systems composed of interconnected molecules and structures, both on the surface and within the cell. These molecular components play vital roles in various physiological processes, including cell adhesion, tissue function, and gene expression regulation through DNA methylation. Understanding how biological systems adapt their properties to fulfill their functions is a significant challenge in biology. At the nanoscale level, the structural, biophysical, and chemical properties of biological systems determine their functionality in response to the surrounding environment. Cells experience mechanical loads and deformations in their natural environment, triggering biochemical changes and interactions with neighboring cells and the extracellular matrix. The process by which cells sense mechanical stimuli and convert them into biochemical signals, known as mechanotransduction, is crucial for normal functioning and development. It involves the transmission of external forces to the cytoskeleton, influencing transcriptional processes and gene expression. AFM offers a powerful tool for quantifying the mechanical properties of cells, including their stiffness and adhesion characteristics. AFM-based force spectroscopy allows for the indentation of cell surfaces and generates force–distance curves that can be analyzed. Alterations in the mechanical properties of cells have been associated with various diseases, such as muscular dystrophies and cancers. AFM has been employed to differentiate between cancerous cells and non-malignant cells based on their mechanical properties, holding great promise for identifying pathological changes in cells and tissues associated with diseases like cancer, arthritis, and cardiovascular disorders. Various studies have compared the mechanical properties of aggressive cancer cells with non-malignant cells using AFM, providing insights into metastasis mechanisms and disease progression. For example, Faria et al. [99] investigated the elastic properties (Figure 11c) of prostate cells at different stages of disease progression and successfully discriminated between benign prostate hyperplasia (BPH), non-invasive prostate cancer cells, and metastatic prostate cancer cells based on their Young's moduli. Li et al. [100] compared the mechanical properties of red blood cells (RBCs) with three aggressive cancer cell types, providing insights into metastasis mechanisms. The results (Figure 11a) showed that RBCs had smaller diameters and lower Young's moduli compared to the cancer cells. Additionally, aggressive cancer cells exhibited lower Young's moduli than indolent cancer cells, providing further insights into metastasis mechanisms. Other studies have explored the mechanical properties of tissues and spheroids associated with pathological conditions, such as ovarian tissues (Figure 11b) [101] and tumor spheroids (Figure 11d) [102], providing insights into physiological and pathological mechanisms.

Lekka et al. [103] measured the stiffness of erythrocytes under physiological conditions using the Hertz model. They observed variations in the Young's modulus distributions among donors, which correlated with factors such as disease type, sex, age, and cigarette smoking. Li et al. [104] examined the elastic properties of individual lymphoma cells and measured the CD20–rituximab binding force on the surface of B-cell lymphoma cells. Rituximab, an anticancer drug used for the treatment of B-cell lymphoma, was linked to the AFM tip to assess the CD20–rituximab binding force on the lymphoma cell surface. The force curves exhibited a clear, sudden peak during retraction [105]. Wang et al. [106] examined the elastic properties of ricin and its interactions with anti-ricin aptamers, revealing distinct binding conformations with unique elastic properties. They developed a method to differentiate specific unbinding pathways by analyzing individual force–extension curves in a multi-pathway system. Another study by Li et al. [107] investigated the impact of methotrexate on the viscoelastic properties of different cell types. AFM indenting with conical and spherical tips was employed to quantitatively measure changes in cellular viscoelastic properties, including Young's modulus and relaxation time. The results demonstrated that methotrexate stimulation significantly reduced both the cellular Young's modulus and the relaxation times (Figure 12a–d). AFM imaging was utilized to visualize the morphological changes induced by methotrexate. Furthermore, AFM has been used to investigate the elastic properties of individual lymphoma cells. In a study conducted

by Wei et al. [108], inverse finite element simulation was used to extract the viscoelastic parameters of living cells based on experimental stress–relaxation curves. This approach allowed for the quantification of the cells' viscoelastic properties. These investigations highlight the potential of AFM in studying the mechanical properties of cancer cells and tissues, providing valuable information for cancer diagnosis, understanding disease progression, and developing new therapeutic approaches, as discussed in the following sections. The combination of AFM with other techniques offers a multidimensional understanding of cancer at the cellular and tissue levels, paving the way for improved cancer detection and treatment strategies.

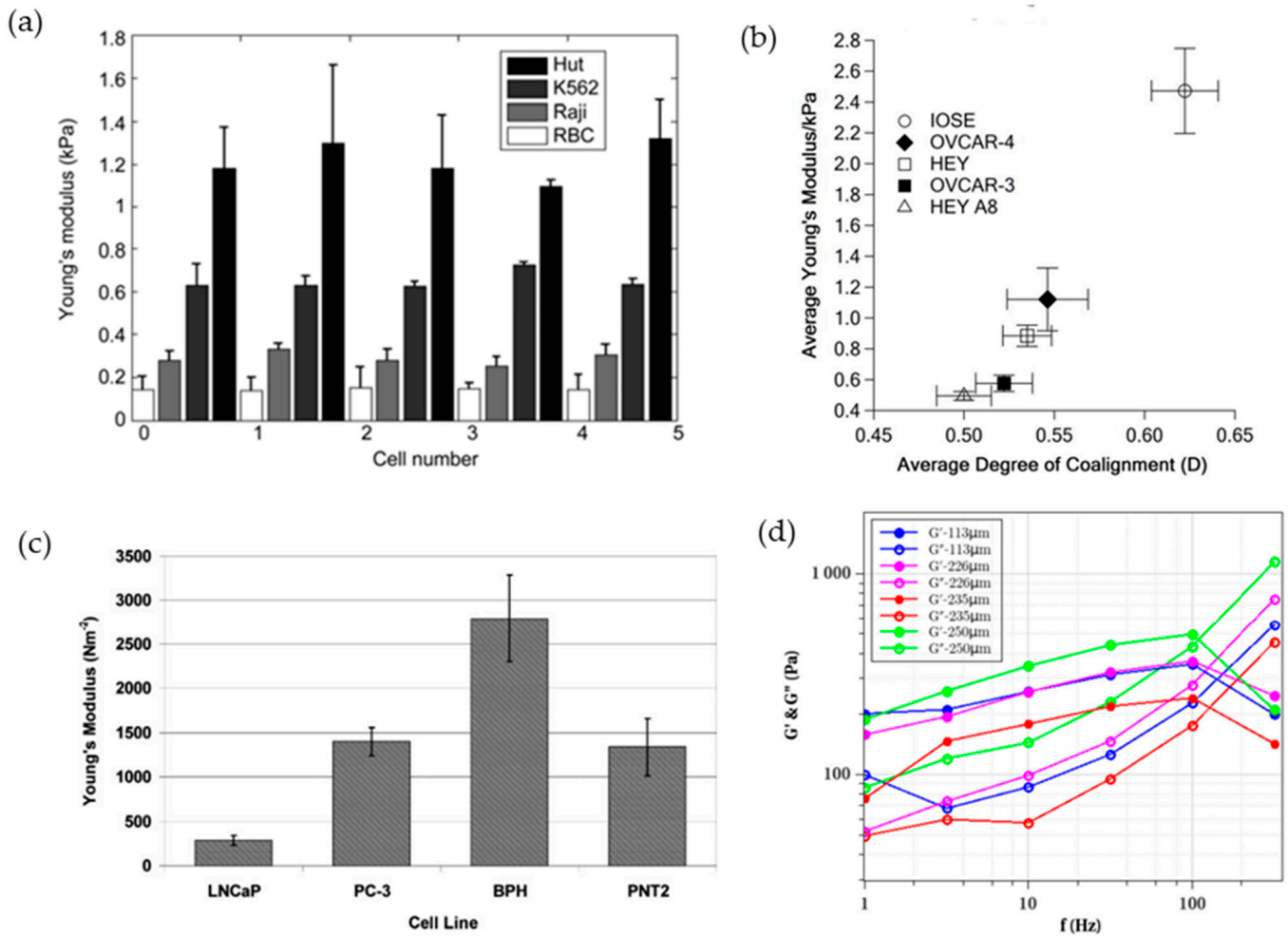


**Figure 11.** (a) Histogram of Young's modulus for RBCs, Raji, Hut, and K562 cells. Reprinted with permission from [100]. (b) Stiffness versus degree of coalignment of F-actin. Reprinted with permission from [101]. (c) Apparent Young's moduli for LNCaP, PC-3, BPH, and PNT2-C2 cells. Reprinted with permission from [99]. (d) Moduli  $G'$  ( $f$ ) and  $G''$  ( $f$ ) as a function of frequency  $f$  (Hz) for different spheroids of various sizes. Reprinted with permission from [102].

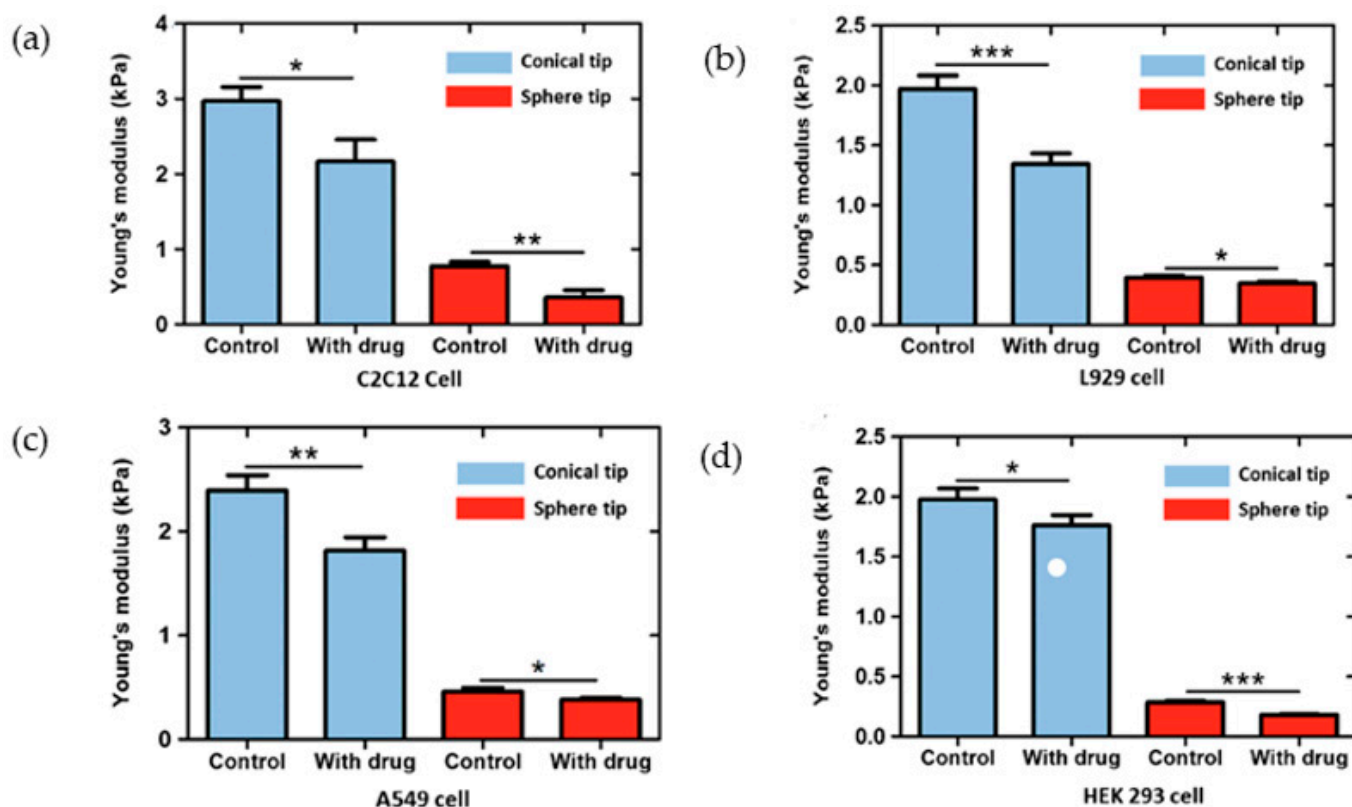


**Figure 12.** (a–d) Young's modulus of C2C12, L929, A549, and HEK 293 cells, respectively, after 24 h of stimulation with methotrexate. (\*  $p < 0.05$ ; \*\*  $p < 0.01$ ; \*\*\*  $p < 0.001$ ) Reprinted with permission from [107].

## 6. Biomarkers

Diseases can give rise to structural and compositional changes in the body, which can serve as early indicators for disease detection. It has been demonstrated that micro- and nano-stiffness alterations can be observed even before visible morphological changes occur. Understanding these changes is crucial for unraveling the underlying physiological mechanisms leading to disease symptoms. Such knowledge not only enables improved symptom management but also establishes the groundwork for effective disease prevention strategies. Therefore, AFM can serve as a valuable tool in studying biomarkers, which are molecules that are indicative of specific diseases or physiological conditions. Biomarkers encompass proteins, nucleic acids, or other detectable molecules present in body fluids, tissues, or cells. Using AFM, one can analyze the topography and mechanical properties of biomolecules. For instance, AFM can measure the stiffness of a protein, providing insights into its folding and stability. This is significant for understanding how environmental changes or interactions with other molecules affect a particular biomarker. By immobilizing the biomarker on a surface and quantifying the force required to detach it, one can determine the strength of the interaction and investigate its modulation by numerous factors. High-resolution imaging enables the identification of the spatial distribution and concentration of specific biomarkers, thereby exploring their presence in different cellular compartments or tissues. AFM transport is particularly valuable for studying biomarkers, since it enables the direct measurement of physical properties and interactions at the individual biomolecular level, which helps in the identification and characterization of biomarkers and can be utilized for diagnostic or prognostic purposes.

### 6.1. Cancer Biomarkers

The role of AFM in characterizing cancer-related biomarkers involves studying biomarker interactions in cancer progression, with cell stiffness serving as a crucial biomarker

for metastatic potential. Li et al. [109] conducted research to explore the connections between cell structure, mechanical properties, and breast cancer. They compared non-malignant (MCF-10A) and malignant (MCF-7) human breast epithelial cell lines. The results (Figure 13a) showed that higher loading rates led to increased stiffness in both cell types, which indicates that cells appear stiffer when probed at higher loading rates, primarily due to the contribution of cell viscosity. At the physiological temperature of 37 °C, the apparent Young's modulus of MCF-10A cells was significantly higher than that of MCF-7 cells at the same loading rate. This implies that non-malignant cells possess greater stiffness compared to malignant cells. The observed difference in cell elasticity was attributed to variations in the organization of the sub-membrane actin structures between the two cell types. MCF-10A cells exhibit well-aligned filamentous structures below the membrane, referred to as stress fibers, which contribute to their higher stiffness. In contrast, MCF-7 cells display less-defined and disorganized filamentous structures, resulting in reduced cell stiffness. These findings suggest a correlation between cell structure, mechanical properties, and breast cancer. In study by Xu et al. [110], non-malignant ovarian cells (IOSE) were compared to ovarian cancer cells (HEY). They found that IOSE cells exhibited higher stiffness than various ovarian cancer cells (HEY) (Figure 13b). This was determined by analyzing the force-indentation curves and calculating the Young's modulus of individual cells. They also examined the relationship between cell stiffness and metastatic potential. HEY A8 cells, which were derived from the same tumor specimen as HEY cells, were found to be more compliant (i.e., less stiff) than HEY cells. This finding is significant, because HEY A8 cells also exhibited higher tumorigenicity and increased invasiveness and migratory activity. This suggests an inverse correlation between cell stiffness and metastatic potential. To understand the molecular basis of the observed differences in cell stiffness, gene expression analysis was performed on HEY and HEY A8 cells. The analysis identified numerous differentially expressed genes between the two cell lines, particularly genes related to cytoskeletal remodeling pathways. These findings support the hypothesis that changes in actin-mediated cytoskeletal remodeling contribute to the differences in cell stiffness. Microscopic examination of the cells confirmed that non-malignant cells had denser and well-aligned F-actin, while ovarian cancer cells displayed less organized and randomly oriented F-actin. The degree of coalignment of F-actin fibers was correlated with cell stiffness, further supporting the relationship between cytoskeletal remodeling and cell stiffness. Li et al. [111] utilized AFM peak force tapping imaging mode to visualize and map CD20 molecules on human lymphoma cells using rituximab-tethered tips. Recognition spots, denoted by green arrows (Figure 13c,d), were observed in the adhesion image, indicating the presence of CD20 molecules on the cell surface. In contrast, normal blood cells from healthy volunteers did not exhibit recognition spots, as they did not express CD20. Quantitative analysis of the cluster sizes of CD20 molecules on the surface of Raji cells was performed using recognition images. The recognition spots were quantitatively analyzed, and the cluster size histogram revealed that CD20 organizations were mainly distributed in the range of 100–4000 nm<sup>2</sup>. Furthermore, they applied PFT imaging to visualize CD20 molecules on cancer cells obtained from a clinical lymphoma patient. Recognition spots were observed in the adhesion image, and the cluster size histogram showed a distribution similar to that observed on Raji cells. AFM imaging allowed for the localization and quantification of CD20 molecules, providing valuable insights into their spatial organization and nanoscale behavior. In another study by Paul et al. [112], AFM-based high-resolution imaging was used to differentiate extracellular vesicles (EVs) derived from colon cancer cells (HCT 116) and healthy colon cells (CCD 18CO). They determined the morphology and ultrastructural characteristics of the EVs, with HCT-116-derived EVs having at least two times higher density compared to CCD-18CO-derived EVs. The CD9-antibody-functionalized AFM tips showed higher rupture forces and frequencies for HCT 116 EVs, indicating a higher density of CD9 molecules on their surface. Spectroscopic techniques confirmed the presence of hyaluronic acid (HA) in HCT 116 EVs, but not in CCD-18CO EVs. The hydrodynamic diameter of the EVs was measured to be around

100 ± 20 nm by dynamic light scattering. The study suggested that HA-enriched EVs could serve as potential biomarkers for colon cancer. Overall, AFM plays a crucial role in characterizing cancer-related biomarkers by investigating biomarker interactions in cancer progression. It enables the study of cell stiffness as a valuable biomarker for metastatic potential and provides insights into the mechanical properties, structural organization, and spatial distribution of molecules in cancer cells and extracellular vesicles. These findings contribute to a better understanding of cancer's mechanisms and the potential development of novel diagnostic and therapeutic approaches.

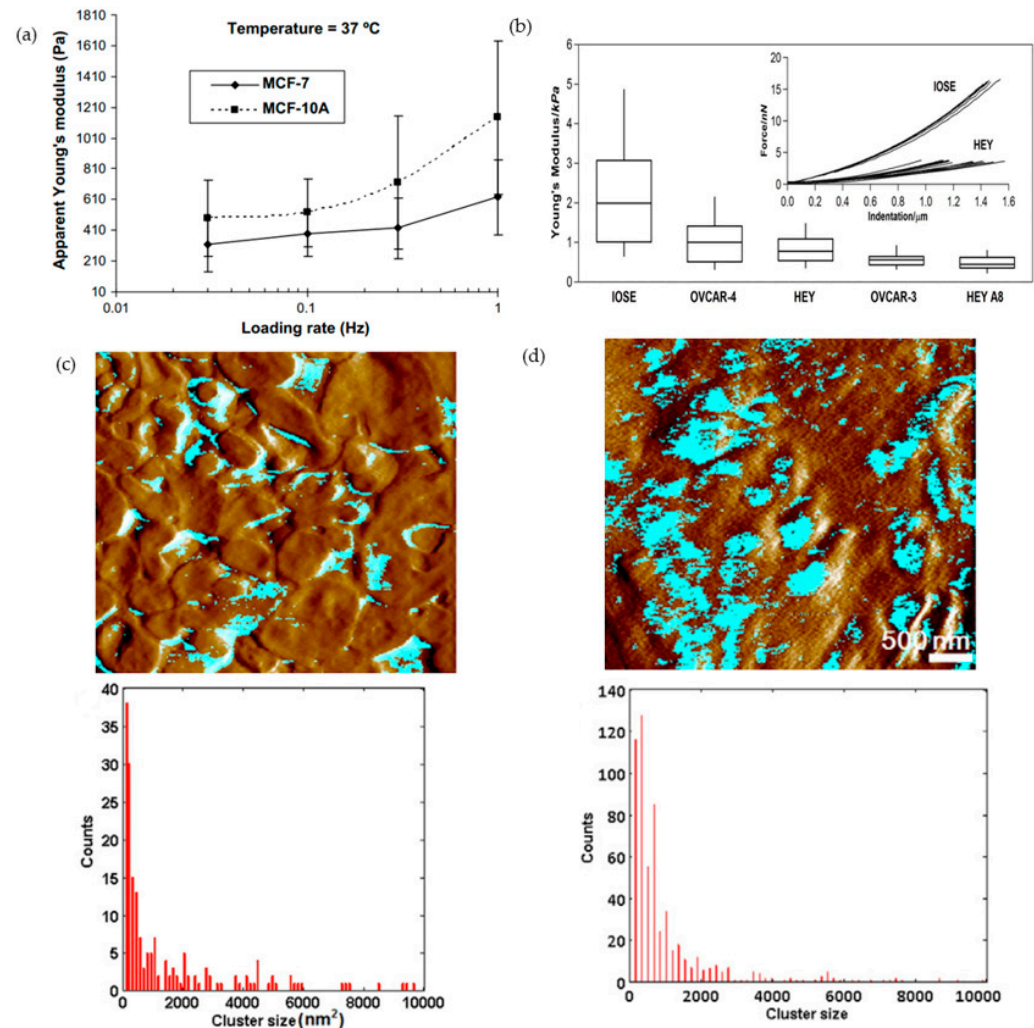


**Figure 13.** (a) Apparent elastic modulus against loading rate for MCF-10A and MCF-7 cells at 37 °C. Reprinted with permission from [109]. (b) Young's modulus of different cells. Reprinted with permission from [110]. (c,d) Overlay of recognition image and the corresponding topographic image and the distribution of recognition spot size of CD20 molecules on lymphoma Raji cell surfaces, without and with rituximab-tethered tips, respectively. Reprinted with permission from [111].

## 6.2. Neurodegenerative Disease Biomarkers

AFM has made significant contributions to the understanding of neurodegenerative disease markers. One area of investigation is the mechanical properties of amyloid fibrils and aggregates. Alzheimer's disease (AD) poses challenges for early detection and accurate diagnosis, leading to extensive research on identifying biomarkers. Understanding the mechanics of brain tissues has emerged as a crucial aspect in diagnosing brain diseases. Park et al. [113] conducted a study using nanoindentation to investigate the viscoelastic properties of human autopsy brain tissues as a potential biomarker for AD. The stress–strain

curves revealed two common factors: a linear relation between stress and strain during the pre-loading phase, and increased stiffness with higher loading frequencies, consistent with soft tissue characteristics. However, brain tissues affected by AD showed moderate slopes during the pre-loading phase, along with greater hysteresis, indicating higher energy dissipation. Comparing the Young's modulus values between normal and AD-affected brain tissues (Figure 14a) showed higher values in normal tissues—by 23.5% for gray matter and 27.9% for white matter. Similar trends were observed in storage modulus, loss modulus, and loss factor measurements. Storage moduli were higher in normal brain tissues, while loss moduli exhibited more overlap. The loss factor indicated a more viscous response in AD-affected brain tissues, especially at lower loading frequencies, suggesting changes in the viscosity and stiffness of extracellular matrix components during AD's progression. Another study by Nirmalraj et al. [114] demonstrated the applicability of AFM for analyzing protein aggregates on RBCs from patients with neurocognitive disorders. The findings highlighted the variations in protein aggregate morphology and assembly patterns, providing insights into the pathophysiological processes associated with AD. They analyzed the size, shape, morphology, assembly patterns, and prevalence of protein aggregates, referred to as physical biomarkers, on red blood cells (RBCs) from patients with neurocognitive disorders—particularly Alzheimer's disease (AD)—and revealed variations in height across RBCs from both patients with disorders and healthy controls. They found that the size, shape, morphology, assembly patterns, and prevalence of protein aggregates on RBCs varied depending on the age and severity of the neurocognitive disorder. They also correlated the AFM measurements of fibrillar aggregates with the A $\beta$ 42/40 ratio in cerebrospinal fluid (CSF), which could be a potential biomarker for AD pathology. The analysis revealed the presence of spherical/annular oligomers, protofibrils, and fibrils on RBCs, with the prevalence of fibrils increasing with the severity of the neurocognitive disorder.

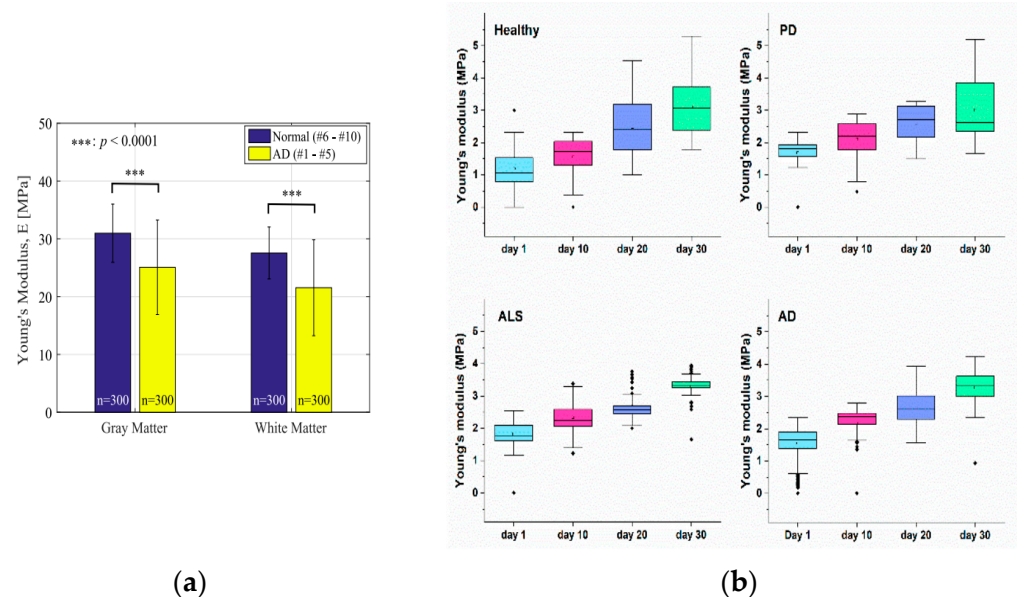


**Figure 14.** (a) Young's modulus (E) of normal and AD-affected human autopsy brain tissues. Reprinted with permission from [113]. (b) Young's modulus of different cells. Reprinted with permission from [115].

Additionally, Strijkova-Kenderova et al. [115] investigated the ultrastructural characteristics of RBCs as a peripheral cell model for specific signatures of neurodegenerative pathologies such as Parkinson's disease (PD), amyotrophic lateral sclerosis (ALS), and AD. They found significant differences in the shape distribution, surface roughness, volume, and Young's modulus between RBCs from patients with neurodegenerative disorders and healthy cells. The percentage of biconcave cells decreased in neurodegenerative disor-

ders, with PD cells exhibiting the lowest proportion of biconcave shape. Differentiated morphology and aging-induced shape transformations distinguished neurodegenerative disorder RBCs from healthy cells. The volume of different cell shapes also differed, allowing for differentiation between AD and other disorders. Surface roughness was lower in neurodegenerative disorder cells but similar between PD, ALS, and AD cells. Increased membrane stiffness, reflected in higher Young's modulus values (Figure 14b), indicated decreased deformability in neurodegenerative disorder RBCs. These findings align with previous studies reporting higher Young's modulus values in PD and AD patients. The study concluded that neurodegenerative disorders lead to distinct alterations in RBCs' surface nanostructure, morphometry, and nanomechanical properties, potentially serving as markers for these disorders. Accumulated misfolded proteins/aggregates and their impact on RBCs' cytoskeleton and lipid bilayer may contribute to the observed morphological transformations.

### 6.3. Infectious Disease Biomarkers

Utilizing AFM to study biomarkers in infectious diseases allows for the investigation of pathogen–host interactions and their impact on biomarker behavior. One such disease is dengue, a mosquito-borne illness caused by dengue virus (DENV) that affects a large number of people worldwide. Unfortunately, the lack of specific treatment options for dengue stems from an incomplete understanding of how viral components interact with cellular structures in the host. To address this knowledge gap, researchers such as Patil et al. [116] have visualized the intramolecular structure of antibodies, while Gilbert et al. [117] demonstrated the capability of AFM to assess the forces and dynamics of molecular interactions in living bacteria. They showed the capability of AFM using vancomycin tips to quantitatively assess the forces and dynamics of the vancomycin/D-Ala-D-Ala interaction (Figure 15a). They also successfully imaged individual D-Ala-D-Ala sites on the division septum of living *Lactococcus lactis* bacteria. Advancements have also been made in studying viral infections using AFM. Rankl et al. [118] investigated the attachment and internalization of human rhinoviruses (HRVs), providing detailed information on virus–receptor interactions at the single-molecule level. Their findings revealed a time-dependent transition from single- to multiple-receptor binding (Figure 15b). The unbinding forces required to detach the virus from the cell membrane increased over several hundred milliseconds. Furthermore, Fantner et al. [119] utilized HS-AFM to enable real-time imaging of live bacterial cells, revealing nanometer-scale resolution and high temporal resolution. They focused on the interaction between antimicrobial peptides and *Escherichia coli* cells, uncovering the multistep process of bacterial cell death (Figure 15c). Investigating the interaction between dengue virus (DENV) capsid protein (C) and low- and very-low-density lipoproteins (LDL and VLDL, respectively) using various techniques, Faustino et al. [120] discovered a specific interaction between DENV C and VLDL, while no interaction was observed with LDL. The results revealed stronger binding forces between DENV C and VLDL (40 pN) compared to LDL (20 pN). This binding was dependent on potassium and involved the N-terminal region of DENV C (Figure 15d,e). They successfully inhibited DENV C–VLDL binding using a peptide drug lead. In addition to their work on DENV, they also investigated the interactions between *Staphylococcus epidermidis* and host proteins absorbed onto biomaterials during biofilm formation. In their research, Herman-Bausier and Dufrêne [121] investigated the binding mechanism of the *S. epidermidis* CWA protein serine-aspartate repeat protein F (SdrF) to type I collagen. They observed that SdrF enables bacterial adhesion to collagen-coated surfaces through both weak and strong bonds (Figure 15f,g). It was also revealed that these bonds involve the A and B regions of SdrF, indicating the protein's dual ligand-binding capability. Notably, the weak and strong bonds exhibited high dissociation rates, suggesting a less stable nature compared to the conventional “dock, lock, and latch” mechanism. These findings shed light on novel ligand-binding mechanisms employed by CWA proteins. Bacterial and viral infections have significant implications for human health, making it essential to study these phenomena at the molecular and

cellular levels using AFM. AFM has been successfully employed in numerous studies to investigate bacterial and viral interactions, cell death processes, intramolecular structures, and the attachment of viruses to host cells. These advancements have greatly contributed to our understanding of infection processes and hold potential for the development of new strategies for diagnosis, treatment, and prevention. For example, Newton et al. [122] introduced a novel AFM technique that quantifies binding events between enveloped viruses and surface receptors on live animal cells, offering insights into early virus–cell interactions. Kiss et al. [123] conducted a study on the topographical and nanomechanical properties of SARS-CoV-2—the virus responsible for the COVID-19 pandemic—revealing its dynamic nature and unique mechanical characteristics (Figure 15h,i). The dynamics of the surface spikes were identified as potentially contributing to the virus’s unusually high infectivity, while its mechanical and self-healing properties may facilitate adaptation to diverse environmental conditions. By leveraging the capabilities of AFM, these studies have expanded our knowledge of bacterial and viral infections, shedding light on their intricate mechanisms and interactions at the molecular level. This information can aid in the development of novel therapeutic approaches, the design of antiviral agents, and the understanding of viral pathogenesis. Ultimately, studying bacterial and viral infections using AFM offers valuable insights that contribute to our ability to combat these infectious diseases effectively.

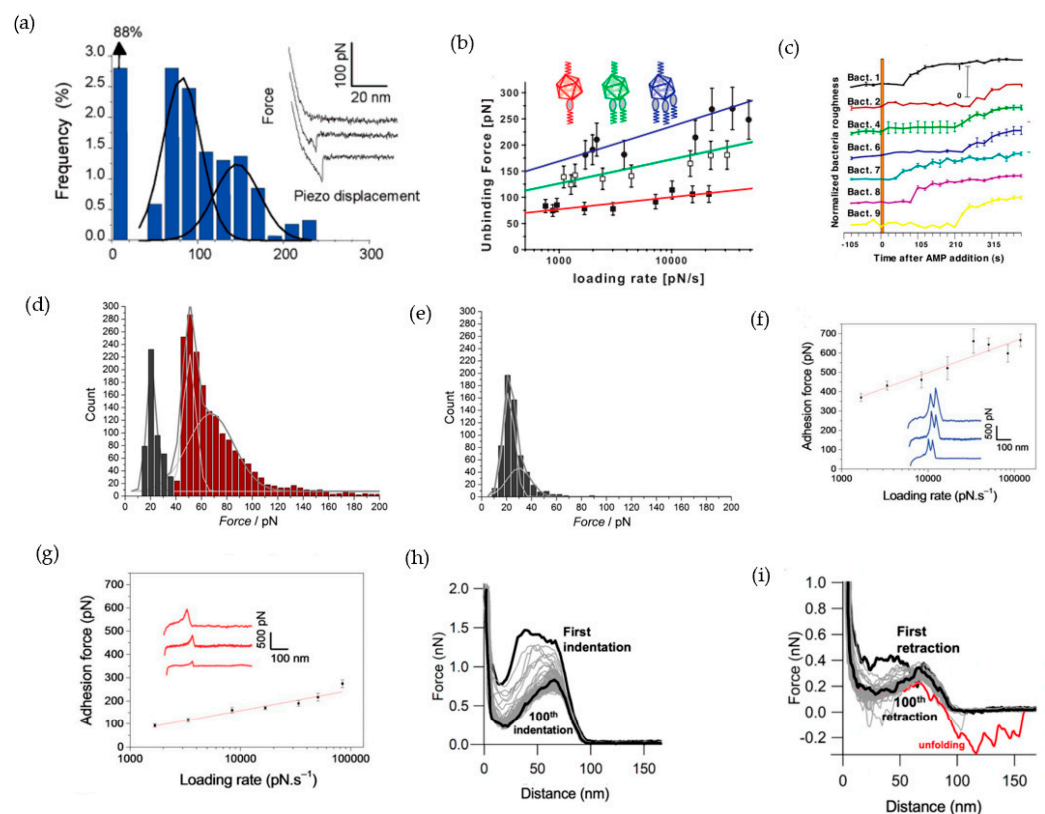


**Figure 15.** (a) Force histogram of adhesion. Reprinted with permission from [117]. (b) Surface variation as a function of time. Reprinted with permission from [118]. (c) Force spectroscopy of the interaction between HRV2 and MBP-V1-8. Reprinted with permission from [119]. (d) Force histogram of the interaction between DENV C and VLDL (e) Force histogram when K<sup>+</sup> is replaced by the same concentration of Na<sup>+</sup>. Reprinted with permission from [120]. (f,g) SdrF–collagen interactions of weak and strong Cn-binding forces, respectively. Reprinted with permission from [121]. (h) Force–distance curves of a single SARS-CoV-2 virion. (i) force–distance curves obtained during retraction. Reprinted with permission from [123].

#### 6.4. Hematological Disorders

Hematological disorders are medical conditions characterized by a propensity for excessive bleeding. The formation of blood clots through fibrinogen polymerization is an essential process to prevent bleeding. However, elevated levels of fibrinogen and erythrocyte aggregation can increase the risk of cardiovascular and cerebrovascular diseases. Previous research has indicated that fibrinogen-induced erythrocyte hyperaggregation is mainly attributed to nonspecific binding. Studies on erythrocyte aggregation in hypertension have suggested the involvement of additional mechanisms. Although AFM combined with force spectroscopy has been used to investigate related systems, the interaction between the entire fibrinogen molecule and its receptors on blood cells has not been specifically examined. Xing et al. [124] conducted a study focusing on a patient with elliptocytosis complicating idiopathic thrombocytopenic purpura (ITP) to investigate the morphological properties of erythrocytes at the nanometer scale. They observed the characteristic biconcave shape and morphological properties of healthy erythrocytes using AFM imaging. In contrast, erythrocytes from the patient group exhibited deformities and surface architecture deformation. Carvalho et al. [125] investigated the binding between fibrinogen and an unidentified receptor on human erythrocyte membranes. They found that fibrinogen-induced erythrocyte aggregation resulted from nonspecific binding to erythrocyte membranes, while platelets possessed a specific fibrinogen integrin receptor. A study by Liu et al. focused on ultrastructural changes in erythrocytes in Waldenström macroglobulinemia (WM), a rare form of lymphoma. They observed significant deformations in the shape and surface membrane of erythrocytes in WM patients compared to healthy controls and patients with multiple myeloma (MM). The WM erythrocytes exhibited ravines, protrusions, and larger particle aggregation on the surface. In contrast, the MM erythrocytes showed smaller deformations and smaller particle aggregation. Liu et al. [126] aimed to investigate the ultrastructural changes in erythrocytes at a nanometer scale in Waldenström macroglobulinemia (WM), a rare form of lymphoma. The results of the study showed significant deformations in the overall shape and surface membrane of erythrocytes in WM patients when compared to healthy controls and MM patients. The healthy erythrocytes exhibited a characteristic biconcave shape, and the ultrastructure showed a regular nanoscale network of membrane proteins. The particles on the surface of healthy erythrocytes were uniform, with a diameter of 10 nm. For the WM patients, the erythrocytes showed dramatic deformations in shape and surface membrane. The cells did not exhibit their regular biconcave shape, and the center of the cell surface was swollen. Ultrastructural examination revealed large ravines and protrusions on the cell surface. Larger particles (greater than 40 nm) were observed on the surface, indicating significant aggregation of membrane proteins. The membrane proteins were reorganized into stripe patterns in one direction. The statistical analysis showed that the length, width, peak, valley, peak-to-valley value, and average surface fluctuation of the WM erythrocytes were significantly different from those of healthy erythrocytes, with increased roughness and peak-to-valley values. The MM patients also exhibited deformations in erythrocyte shape and surface membrane. The cells did not exhibit their regular biconcave shape, and small holes were observed on the cell surface. The particles on the surface were smaller than those observed in WM erythrocytes, and their distribution was heterogeneous. Li et al. [127] used AFM combined with magnetic bead cell isolation to measure the viscoelastic properties of human primary B lymphocytes. They isolated B lymphocytes from healthy volunteers and quantitatively measured the instantaneous modulus and relaxation time of living B lymphocytes. The results showed that the instantaneous modulus of normal human B lymphocytes was 2–3 kilopascals (kPa), and the relaxation times ranged from 0.03 to 0.06 s and from 0.35 to 0.55 s. Jembrek et al. [128] investigated the cellular and molecular consequences of oxidative injury induced by hydrogen peroxide ( $H_2O_2$ ) in P19 neurons to understand the neuroprotective mechanisms of quercetin beyond its antioxidant activity. It was observed that the viability of P19 neurons decreased in a concentration-dependent manner when exposed to  $H_2O_2$ , while quercetin treatment did not decrease cell survival even at high concentrations. Quercetin treatment prevented the

downregulation of Bcl-2 and the upregulation of p53. Additionally, they also analyzed the expression of glyceraldehyde-3-phosphate dehydrogenase (GAPDH), a metabolic enzyme with non-glycolytic functions that is involved in oxidative stress sensing and cell death induction. While H<sub>2</sub>O<sub>2</sub> did not affect GAPDH expression, quercetin treatment led to pronounced upregulation of GAPDH. The neurons exposed to H<sub>2</sub>O<sub>2</sub> exhibited an irregular circular shape and degenerated cell bodies, while those treated with quercetin displayed a more regular morphology resembling that of control neurons. Feng et al. [129] investigated the nanomechanical properties of extracellular vesicles (EVs) from the fluid biopsies of clinical hematological cancer patients to understand the role of EV mechanics in the development of hematological cancer. The results showed significant differences in EV mechanics between multiple myeloma patients, lymphoma patients, and healthy volunteers. The mechanical properties of EVs were found to be associated with their geometric features, such as height, radius, and deformation degree. Furthermore, the study demonstrated dynamic changes in the mechanical properties of EVs during the development of hematological cancer. Multiple myeloma patients showed smaller Young's moduli and viscous coefficients of EVs in the bone marrow compared to the blood, while lymphoma patients showed the opposite trend. The mechanical and geometric alterations of EVs were highly heterogeneous for different types of fluid biopsies and hematological cancers. By utilizing AFM in these studies, the researchers gained insights into the morphological, mechanical, and ultrastructural properties of erythrocytes, the binding mechanisms between fibrinogen and erythrocytes, the viscoelastic properties of B lymphocytes, the effects of quercetin on neuronal morphology, and the mechanical characteristics of EVs in hematological cancer patients. These findings contribute to our understanding of bleeding disorders, cellular behaviors, and the pathogenesis of hematological cancers, facilitating the development of potential treatments and diagnostic strategies.

## 7. The Multifaceted Applications of AFM in Drug Therapy

Understanding the interactions between drugs and their target molecules is crucial for optimizing drug molecule design and enhancing their effectiveness in the field of drug discovery and development. The efficacy of a drug is closely linked to its ability to interact with specific target molecules. Traditionally, techniques such as binding assays and spectroscopic methods have been employed to investigate these interactions, but they often provide limited insights into the mechanical properties and forces involved. To overcome these limitations, AFM—a high-resolution imaging and force measurement technique—offers a unique opportunity to probe drug–target interactions at the single-molecule level. It provides valuable information on the strength of these interactions and their contributing factors. By studying the interactions between drugs and their target molecules, one can assess their strength and analyze various influencing factors, contributing to the optimization of drug molecule design and enhancing their effectiveness. Furthermore, AFM plays a crucial role in investigating drug delivery to cells or tissues. By performing high-resolution imaging, AFM enables the tracking of drug molecules' location and distribution within the sample, shedding light on their uptake by cells or tissues. This knowledge aids in the development of improved drug-delivery strategies and enhances targeted delivery to specific cells or tissues, potentially improving therapeutic outcomes. Additionally, AFM can be used to monitor the efficiency of drug therapy by measuring the mechanical properties of cells or tissues before and after drug treatment, providing more effective treatment approaches. In the context of chemotherapy, the targeted release of anticancer drugs at tumor sites to induce cancer cell death is vital. However, the impact of drugs on the mechanical properties of cancer cells is not yet fully understood. Moreover, the stiffness of tumor tissue is significantly influenced by factors such as tumor stage, invasiveness, and location within the tumor, which are related to the deposition of extracellular matrix and affect cellular behavior at the single-cell level. Consequently, studying the impact of hypoxia on cellular structure and its relationship with drug effects provides essential insights into the tumor microenvironment's dynamics and its influence

on treatment outcomes. In this section, we explore the multifaceted applications of AFM in drug therapy. This encompasses the study of drug–target interactions, drug delivery, monitoring treatment efficiency, and investigating binding mechanisms. AFM offers a powerful tool to unravel the intricacies of drug interactions and optimize therapeutic strategies in the field of drug discovery and development.

### 7.1. Investigating Drug Delivery

AFM plays a crucial role in investigating drug delivery to cells or tissues. By performing high-resolution imaging, AFM enables the tracking of drug molecules' location and distribution within the sample, shedding light on their uptake by cells or tissues. This knowledge aids in the development of improved drug-delivery strategies and enhances targeted delivery to specific cells or tissues, potentially improving therapeutic outcomes. For example, Zhang et al. [130] conducted a study on the binding mechanism of diosmetin to human serum albumin (HSA). The topographic image of HSA molecules absorbed onto mica was observed. By averaging the width of 50 single HSA molecules, the mean width and height of individual HSA molecules was determined to be  $25 \pm 4.5$  nm and  $4.1 \pm 2.6$  nm, respectively. Upon interaction with diosmetin, the HSA molecule appeared to be more swollen on the mica substrate, and flocculation or aggregation of HSA molecules could be observed. The mean width and height of the molecules increased to  $102 \pm 9.1$  nm and  $12.5 \pm 3.0$  nm, respectively—significantly larger than the original HSA dimensions. This change in size suggested that there was an interaction between HSA and diosmetin. The interaction with diosmetin altered the microenvironment around the HSA molecule, exposing it to a more hydrophobic environment. To minimize the unfavorable factors and stabilize the structure, the HSA molecule reduced its surface area in contact with water by undergoing molecular aggregation. This resulted in the observation of larger molecules on the mica substrate. The AFM analysis thus confirmed the presence of hydrophobic interactions between HSA and diosmetin. Similarly, Domingues et al. [131] investigated the interaction between rBPI21—an antimicrobial peptide—and two types of bacteria: *Escherichia coli* (Gram-negative) and *Staphylococcus aureus* (Gram-positive). They found that rBPI21 caused changes in the bacterial membranes. In *E. coli*, the peptide led to membrane vesiculation and flattening at low concentrations, progressing to complete membrane disruption and bacterial lysis at higher concentrations. In *S. aureus*, rBPI21 increased the surface roughness, disrupted the bacterial structure, and caused lysis. They also studied the influence of soluble LPS on the interaction between rBPI21 and the bacteria, observing that LPS reduced the binding frequency of rBPI21 to both *E. coli* and *S. aureus*. In the case of *S. aureus*, the binding forces were shifted to lower values in the presence of LPS, indicating the involvement of another ligand—potentially lipoteichoic acid or wall teichoic acid. In another study by Rajendran et al. [132], new insights into the binding of drug–quadruplex intermediates was presented. They proposed molecular mechanisms involved in drug-induced quadruplex folding. The ligand used in the study was bisquinolinium pyridine dicarboxamide bearing a biotin linker (PDC-biotin). DNA origami frames were employed to control the DNA sequences and investigate tetramolecular antiparallel and (3 + 1)-type structures. They observed small-molecule-induced conformational switching using AFM and confirmed the presence of the ligand in the intermediate structures through streptavidin localization. The study also examined the formation of G-hairpin and G-triplex intermediates induced by the ligand. These findings provide valuable insights into drug–intermediate binding and have implications for the development of novel anticancer drugs targeting G-rich regions. Thus, AFM serves as a valuable tool in investigating drug delivery, molecular interactions, and conformational changes. It enables high-resolution imaging, facilitating the tracking of drug molecules and providing insights into their uptake by cells or tissues.

### 7.2. Monitoring Treatment Efficiency

AFM has the potential to monitor the efficiency of drug therapy by assessing the mechanical properties of cells or tissues before and after treatment. The impact of drugs on the mechanical properties of cancer cells, in particular, is not yet fully understood. Factors such as tumor stage, invasiveness, and location within the tumor significantly influence the stiffness of tumor tissue, which is related to the deposition of extracellular matrix and affects cellular behavior at the single-cell level. Understanding the effect of hypoxia on cellular structure and its relationship with drug efficacy provides crucial insights into tumor microenvironment dynamics and treatment outcomes. In a study by Li et al. [133], the effects of different drugs on the mechanical properties of lymphoma (Figure 16e,f) were investigated, and it was revealed that rituximab significantly enhanced the efficacy of chemotherapy drugs in inducing cell death. Similarly, Ren et al. [134] examined the effects of eight anticancer drugs on the mechanical properties of human prostate cancer cells (PC-3) using a control-based nanoindentation measurement protocol on an AFM. By measuring the Young's modulus of PC-3 cells treated with the drugs, it was observed that the drugs substantially increased the Young's modulus, with a more pronounced effect at higher force loading rates. Two distinct patterns were observed: one group of drugs (disulfiram, paclitaxel, and MK-2206) showed a relatively unchanged exponent coefficient of the frequency–modulus function, while the other group (Celebrex, BAY, tomatine, TPA, and valproic acid) significantly increased the exponential rate. The study suggested that the changes in mechanical properties may be correlated with the ability of cancer cells to metastasize, highlighting the potential of physical properties as targets for the development of anticancer drugs. In another study by Alhalhooly et al. [135], the impact of the drugs gemcitabine, doxorubicin, vincristine, and mitoxantrone on the mechanical properties of four cancer cell lines (pancreas, breast, glioblastoma, and prostate) was investigated, and it was found that brain, breast, and pancreatic cancer cells exhibited a decrease in stiffness, while prostate cancer cells showed increased stiffness (Figure 16a,b). This was attributed to drug-induced disruption of the cytoskeletal structure. Also, it was noted that the rate of stiffness change was reduced by up to twofold in hypoxia, suggesting a relationship between cellular stiffness and drug resistance in the hypoxic tumor microenvironment. Overall, the assessment of cellular mechanical properties through AFM provides valuable insights into the efficacy of drug therapy. Studies have demonstrated that certain drugs can alter the mechanical properties of cancer cells, potentially influencing their behavior and response to treatment. Understanding these mechanical changes can contribute to the development of novel therapeutic strategies and, ultimately, improve treatment outcomes.

### 7.3. Investigating Binding Mechanisms

AFM plays a significant role in investigating the binding mechanisms between drugs and their target molecules. By studying nanoscale interactions, AFM can provide insights into specific binding mechanisms and alterations in the geometric characteristics of molecules upon drug stimulation. These findings have implications for the development of more precise and efficient drugs. For instance, Taranta, Bizzarri, and Cannistraro [136] conducted research on the impact of a P53 drug on azurin, revealing unbinding forces of approximately 70 pN (Figure 16c,d). In another study by Zhang et al. [137], the ability of the drug LHRH-PE40 to recognize LHRH-Rs on the surface of living cells was compared to that of LHRH and LHRH-R using dynamic force spectroscopy, revealing that the LHRH moiety retained its specific recognition capability for LHRH-R, suggesting that the recombinant protein LHRH-PE40 holds promise as a targeted drug. This indicates that the LHRH analogue exhibits a high affinity for its target receptor, making it a potential candidate for effective carcinoma treatment. The study also provided insights into the specific binding mechanisms between the analogue and the receptor, which could guide the development of more precise and efficient drugs in the future. Furthermore, Xiao et al. [138] studied the interaction of metformin with transforming growth factor- $\beta$ 1 (TGF- $\beta$ 1), a molecule involved in the development of various diseases. Through AFM, they demonstrated that metformin

inhibits the binding of TGF- $\beta$ 1 to its receptor, T $\beta$ RII, by conducting TGF- $\beta$ 1-T $\beta$ RII binding force measurements on live cells. The force distribution histogram obtained from the experiments exhibited a single peak, indicating the measurement of single-molecule forces. In cells treated with metformin at a concentration of 50  $\mu$ M, the binding forces between TGF- $\beta$ 1 and T $\beta$ RII on the cell surface were similar to those in the control group. However, metformin significantly reduced the binding probabilities, from  $21.7 \pm 3.5\%$  to  $9.9 \pm 1.2\%$ . This reduction in binding probability was comparable to the results obtained with the TGF- $\beta$ 1 antibody treatment ( $6.4 \pm 1.9\%$ ). Additionally, Li et al. [139] explored the nanoscale interactions between plasmid DNAs and drugs (methotrexate and cisplatin) and demonstrated significant alterations in the geometric characteristics of the plasmid DNAs upon drug stimulation. Moreover, Yun et al. [140] investigated the biomechanical properties of HeLa cells before and after treatment with docetaxel. The AFM images revealed differences in cell morphology between control and docetaxel-treated cells. The untreated cells exhibited lamellipodia, while the treated cells showed a significant reduction in lamellipodia and an increased apparent height. Measurements of cell height indicated that docetaxel-treated cells had a significantly higher average height ( $3.73 \pm 0.53 \mu\text{m}$ ) compared to untreated cells ( $2.43 \pm 0.59 \mu\text{m}$ ). This suggests that docetaxel treatment led to changes in cell structure. The surface brush length, viscosity factor, and adhesion work were significantly reduced in docetaxel-treated cells compared to untreated cells. The brush length decreased by approximately 250 nm. The reduced brush length and adhesion work suggest alterations in cell surface properties. Lastly, Song et al. [141] studied the interaction between the type 2 diabetes drug pioglitazone and the outer mitochondrial membrane protein mitoNEET (mNT) using AFM. They examined the unfolding pathways and kinetics of mNT in the presence and absence of pioglitazone. Without pioglitazone, mNT unfolded in a one-step process, with a contour length change of  $12.7 \pm 1.2 \text{ nm}$ . Interestingly, multiple peaks of 18 nm were observed from a different region of the protein. On the other hand, when pioglitazone was present in excess, a smaller force peak of 13 nm was observed at  $106 \pm 59 \text{ pN}$ . The unfolding force of mNT was found to be dependent on the loading rate, and a linear relationship was observed. The off rate ( $k_{\text{off}}$ ) for mNT was measured to be  $1.4 \text{ s}^{-1}$ , while for the mNT-pioglitazone complex it was  $4.0 \text{ s}^{-1}$ . Stepwise unfolding events of mNT were also observed, including a two-step unfolding event with peaks of 8 nm and 5 nm. Pioglitazone binding had significant effects on the kinetic stability of the protein. It decreased the off rate of the 5 nm peak from the metal cluster by 10-fold and the off rate of the 8 nm peak from the protein structure outside the cluster by 3-fold. Furthermore, the rupture of the labile Fe-N bond in the metal cluster resulted in stepwise force peaks, and pioglitazone had a lesser effect on the kinetic stability of the partially ruptured cluster. Pioglitazone was found to increase the kinetic stability of the metal cluster by stabilizing the Fe(III)-N(His87) bond, inhibiting its release/transfer. These findings highlight the influence of pioglitazone on the unfolding pathways, kinetics, and kinetic stability of mNT, particularly targeting the metal cluster. In conclusion, AFM-based investigations play a pivotal role in unraveling the binding mechanisms between drugs and their target molecules. These studies provide crucial insights into nanoscale interactions and the consequent alterations in molecular characteristics induced by drug stimulation. Such knowledge holds immense promise for the development of more precise and efficient drugs in the future.

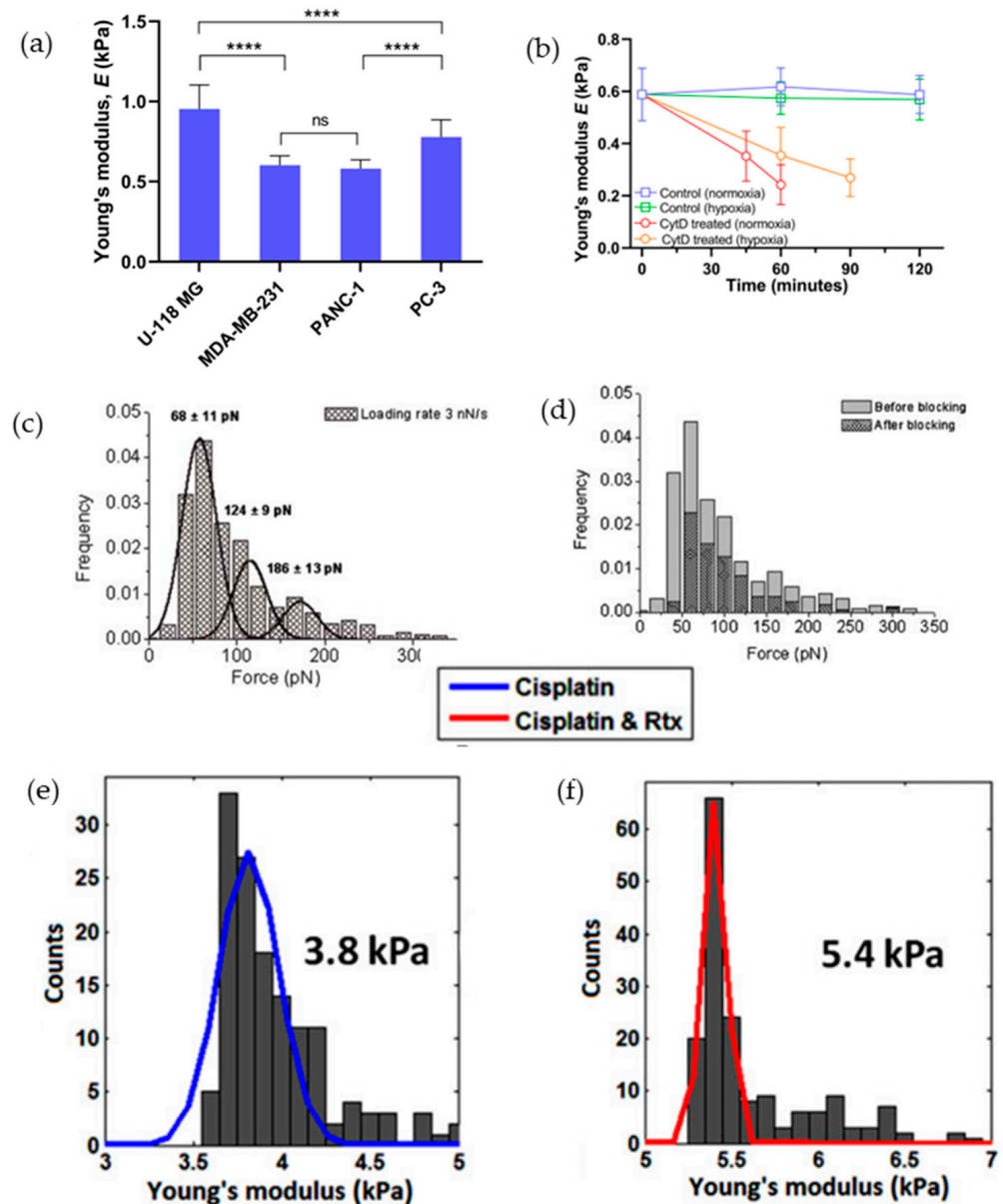


**Figure 16.** (a) Young's modulus ( $E$ ) compared for four different cancer cell lines (\*\*\*\*  $p < 0.0001$ ). (b) Time trace of Young's modulus. (a,b) Reprinted with permission from [135]. (c) Force diagram of unbinding events. (d) Unbinding force distribution comparison of before and after blocking the p53 monolayer. (c,d) Reprinted with permission from [136]. (e,f) Histogram of Young's moduli of cisplatin (e) and cisplatin and Rtx (f). Reprinted with permission from [133].

## 8. Conclusions and Perspective

The field of biology has undergone a remarkable transformation with the advent of AFM, which allows for the characterization and manipulation of various interfaces at the molecular level. It not only enables high-resolution imaging of biological surfaces, but also facilitates the measurement of biomolecular interactions. The use of force–distance curves generated by AFM holds tremendous potential for unraveling both inter- and intramolecular interactions under physiological conditions and investigating mechanical properties. By modifying the AFM tip, one can explore a wide range of interactions, from molecules to cells. The force spectroscopic modes of AFM provide a valuable tool for characterizing real-time molecular interaction dynamics. However, despite these advancements, there are still several technical challenges when it comes to investigating living cells at the single-molecule level. One of the key challenges is distinguishing between specific and nonspecific

binding within the complex cellular environment. This poses difficulties when attempting to measure specific biomolecular interaction forces accurately. In summary, AFM-based measurements will continue to play a crucial role in future biological research, significantly enhancing our understanding of the structures and properties of various cellular molecular mechanisms at the single-molecule level. The integration of AFM with other techniques holds great promise for providing further insights into transport phenomena in biological systems and may lead to the development of novel therapeutic strategies for various diseases. Future research in this field is expected to focus on the development of new AFM-based techniques for studying molecular interactions in biological systems and integrating AFM with other analytical techniques to gain a more comprehensive understanding of these interactions.

**Funding:** This research was partially funded by the US National Science Foundation (ECCS 2010875).

**Data Availability Statement:** Data sharing is not applicable here, as we did not generate any data.

**Conflicts of Interest:** The authors affirm that they do not possess any conflict of interest.

## References

1. Steffens, C.; Leite, F.L.; Bueno, C.C.; Manzoli, A.; De Paula Herrmann, P.S. Atomic force microscopy as a tool applied to nano/biosensors. *Sensors* **2012**, *12*, 8278–8300. [[CrossRef](#)] [[PubMed](#)]
2. Binnig, G.; Quate, C.F.; Gerber, C. Atomic force microscope. *Phys. Rev. Lett.* **1986**, *56*, 930. [[CrossRef](#)] [[PubMed](#)]
3. Zemła, J.; Danilkiewicz, J.; Orzechowska, B.; Pabijan, J.; Seweryn, S.; Lekka, M. Atomic force microscopy as a tool for assessing the cellular elasticity and adhesiveness to identify cancer cells and tissues. *Semin. Cell Dev. Biol.* **2018**, *73*, 115–124. [[CrossRef](#)] [[PubMed](#)]
4. Lyubchenko, Y.L.; Shlyakhtenko, L.S. AFM for analysis of structure and dynamics of DNA and protein–DNA complexes. *Methods* **2009**, *47*, 206–213. [[CrossRef](#)] [[PubMed](#)]
5. Schön, P. Imaging and force probing RNA by atomic force microscopy. *Methods* **2016**, *103*, 25–33. [[CrossRef](#)]
6. Sajja, S.; Chandler, M.; Fedorov, D.; Kasprzak, W.K.; Lushnikov, A.; Viard, M.; Shah, A.; Dang, D.; Dahl, J.; Worku, B. Dynamic behavior of RNA nanoparticles analyzed by AFM on a mica/air interface. *Langmuir* **2018**, *34*, 15099–15108. [[CrossRef](#)]
7. Connell, S.D.; Smith, D.A. The atomic force microscope as a tool for studying phase separation in lipid membranes. *Mol. Membr. Biol.* **2006**, *23*, 17–28. [[CrossRef](#)]
8. Puech, P.-H.; Poole, K.; Knebel, D.; Muller, D.J. A new technical approach to quantify cell–cell adhesion forces by AFM. *Ultramicroscopy* **2006**, *106*, 637–644. [[CrossRef](#)]
9. Allison, D.P.; Mortensen, N.P.; Sullivan, C.J.; Doktycz, M.J. Atomic force microscopy of biological samples. *Wiley Interdiscip. Rev. Nanomed. Nanobiotechnol.* **2010**, *2*, 618–634. [[CrossRef](#)]
10. Dufrêne, Y.F. Sticky microbes: Forces in microbial cell adhesion. *Trends Microbiol.* **2015**, *23*, 376–382. [[CrossRef](#)]
11. Wagh, A.A.; Roan, E.; Chapman, K.E.; Desai, L.P.; Rendon, D.A.; Eckstein, E.C.; Waters, C.M. Localized elasticity measured in epithelial cells migrating at a wound edge using atomic force microscopy. *Am. J. Physiol.-Lung Cell. Mol. Physiol.* **2008**, *295*, L54–L60. [[CrossRef](#)]
12. Luo, Q.; Kuang, D.; Zhang, B.; Song, G. Cell stiffness determined by atomic force microscopy and its correlation with cell motility. *Biochim. Biophys. Acta (BBA)-Gen. Subj.* **2016**, *1860*, 1953–1960. [[CrossRef](#)]
13. Fang, T.; Alvelid, J.; Spratt, J.; Ambrosetti, E.; Testa, I.; Teixeira, A.I. Spatial regulation of T-cell signaling by programmed death-ligand 1 on wireframe DNA origami flat sheets. *ACS Nano* **2021**, *15*, 3441–3452. [[CrossRef](#)]
14. Shi, X.; Zhang, X.; Xia, T.; Fang, X. Living cell study at the single-molecule and single-cell levels by atomic force microscopy. *Nanomedicine* **2012**, *7*, 1625–1637. [[CrossRef](#)]
15. Zhang, Q.; Yang, J.; Tillieux, S.; Guo, Z.; Natividade, R.d.S.; Koehler, M.; Petitjean, S.; Cui, Z.; Alsteens, D. Stepwise Enzymatic-Dependent Mechanism of Ebola Virus Binding to Cell Surface Receptors Monitored by AFM. *Nano Lett.* **2022**, *22*, 1641–1648. [[CrossRef](#)]
16. Neaves, K.J.; Cooper, L.P.; White, J.H.; Carnally, S.M.; Dryden, D.T.; Edwardson, J.M.; Henderson, R.M. Atomic force microscopy of the EcoKI Type I DNA restriction enzyme bound to DNA shows enzyme dimerization and DNA looping. *Nucleic Acids Res.* **2009**, *37*, 2053–2063. [[CrossRef](#)]
17. Clark, C.G.; Sun, Z.; Meiningner, G.A.; Potts, J.T. Atomic force microscopy to characterize binding properties of  $\alpha 7$ -containing nicotinic acetylcholine receptors on neurokinin-1 receptor-expressing medullary respiratory neurons. *Exp. Physiol.* **2013**, *98*, 415–424. [[CrossRef](#)]
18. Bergler, F.; Fuentes, C.; Kadir, M.F.; Navarrete, C.; Supple, J.; Barrera, N.P.; Edwardson, J.M. Activation of P2X4 receptors induces an increase in the area of the extracellular region and a decrease in receptor mobility. *FEBS Lett.* **2020**, *594*, 4381–4389. [[CrossRef](#)]
19. Murrough, J.W.; Huang, Y.; Hu, J.; Henry, S.; Williams, W.; Gallezot, J.-D.; Bailey, C.R.; Krystal, J.H.; Carson, R.E.; Neumeister, A. Reduced amygdala serotonin transporter binding in posttraumatic stress disorder. *Biol. Psychiatry* **2011**, *70*, 1033–1038. [[CrossRef](#)]

20. Ruozi, B.; Tosi, G.; Leo, E.; Vandelli, M.A. Application of atomic force microscopy to characterize liposomes as drug and gene carriers. *Talanta* **2007**, *73*, 12–22. [[CrossRef](#)]
21. Cardoso, F.L.; Brites, D.; Brito, M.A. Looking at the blood–brain barrier: Molecular anatomy and possible investigation approaches. *Brain Res. Rev.* **2010**, *64*, 328–363. [[CrossRef](#)] [[PubMed](#)]
22. Zhou, Y.; Peng, Z.; Seven, E.S.; Leblanc, R.M. Crossing the blood-brain barrier with nanoparticles. *J. Control. Release* **2018**, *270*, 290–303. [[CrossRef](#)] [[PubMed](#)]
23. Fotiadis, D. Atomic force microscopy for the study of membrane proteins. *Curr. Opin. Biotechnol.* **2012**, *23*, 510–515. [[CrossRef](#)] [[PubMed](#)]
24. Dhar-Chowdhury, P.; Malester, B.; Rajacic, P.; Coetzee, W. The regulation of ion channels and transporters by glycolytically derived ATP. *Cell. Mol. Life Sci.* **2007**, *64*, 3069–3083. [[CrossRef](#)] [[PubMed](#)]
25. Alessandrini, A.; Facci, P. Phase transitions in supported lipid bilayers studied by AFM. *Soft Matter* **2014**, *10*, 7145–7164. [[CrossRef](#)]
26. Viles, J.H. Imaging Amyloid- $\beta$  Membrane Interactions; Ion-channel pores and Lipid-Bilayer Permeability in Alzheimer’s Disease. *Angew. Chem.* **2023**, e202215785. [[CrossRef](#)]
27. Yacoot, A.; Koenders, L. Aspects of scanning force microscope probes and their effects on dimensional measurement. *J. Phys. D Appl. Phys.* **2008**, *41*, 103001. [[CrossRef](#)]
28. Meng, L.; Huang, T.; Wang, X.; Chen, S.; Yang, Z.; Ren, B. Gold-coated AFM tips for tip-enhanced Raman spectroscopy: Theoretical calculation and experimental demonstration. *Opt. Express* **2015**, *23*, 13804–13813. [[CrossRef](#)]
29. Chan, K.A.; Kazarian, S.G. Tip-enhanced Raman mapping with top-illumination AFM. *Nanotechnology* **2011**, *22*, 175701. [[CrossRef](#)]
30. Sadewasser, S.; Villanueva, G.; Plaza, J. Modified atomic force microscopy cantilever design to facilitate access of higher modes of oscillation. *Rev. Sci. Instrum.* **2006**, *77*, 073703. [[CrossRef](#)]
31. Moore, S.I.; Ruppert, M.G.; Yong, Y.K. AFM cantilever design for multimode Q control: Arbitrary placement of higher order modes. *IEEE/ASME Trans. Mechatron.* **2020**, *25*, 1389–1397. [[CrossRef](#)]
32. Joshi, M.; Rao, V.R.; Mukherji, S. A novel technique for microfabrication of ultra-thin affinity cantilevers for characterization with an AFM. *J. Micromechanics Microengineering* **2010**, *20*, 125007. [[CrossRef](#)]
33. Liu, J.; Jiang, Y.; Grierson, D.S.; Sridharan, K.; Shao, Y.; Jacobs, T.D.; Falk, M.L.; Carpick, R.W.; Turner, K.T. Tribochemical wear of diamond-like carbon-coated atomic force microscope tips. *ACS Appl. Mater. Interfaces* **2017**, *9*, 35341–35348. [[CrossRef](#)]
34. Yu, F.; Liu, J.; Zhang, X.; Lin, A.-L.; Khan, N.; Pan, Y.; Gao, N.; Zou, Q.; Jeon, J. Design, fabrication, and characterization of polymer-based cantilever probes for atomic force microscopes. *J. Vac. Sci. Technol. B Nanotechnol. Microelectron. Mater. Process. Meas. Phenom.* **2016**, *34*, 06KI01. [[CrossRef](#)]
35. Wilson, N.R.; Macpherson, J.V. Carbon nanotube tips for atomic force microscopy. *Nat. Nanotechnol.* **2009**, *4*, 483–491. [[CrossRef](#)]
36. Meyer, G.; Amer, N.M. Novel optical approach to atomic force microscopy. *Appl. Phys. Lett.* **1988**, *53*, 1045–1047. [[CrossRef](#)]
37. Tortonese, M.; Barrett, R.; Quate, C. Atomic resolution with an atomic force microscope using piezoresistive detection. *Appl. Phys. Lett.* **1993**, *62*, 834–836. [[CrossRef](#)]
38. Villanueva, G.; Plaza, J.; Montserrat, J.; Perez-Murano, F.; Bausells, J. Crystalline silicon cantilevers for piezoresistive detection of biomolecular forces. *Microelectron. Eng.* **2008**, *85*, 1120–1123. [[CrossRef](#)]
39. Shiba, Y.; Ono, T.; Minami, K.; Esashi, M. Capacitive AFM probe for high speed imaging. *IEEJ Trans. Sens. Micromachines* **1998**, *118*, 647–651. [[CrossRef](#)]
40. Ramachandran, S.; Teran Arce, F.; Lal, R. Potential role of atomic force microscopy in systems biology. *Wiley Interdiscip. Rev. Syst. Biol. Med.* **2011**, *3*, 702–716. [[CrossRef](#)]
41. Gaboriaud, F.; Dufrêne, Y.F. Atomic force microscopy of microbial cells: Application to nanomechanical properties, surface forces and molecular recognition forces. *Colloids Surf. B Biointerfaces* **2007**, *54*, 10–19. [[CrossRef](#)] [[PubMed](#)]
42. Weymouth, A.J. Non-contact lateral force microscopy. *J. Phys. Condens. Matter* **2017**, *29*, 323001. [[CrossRef](#)] [[PubMed](#)]
43. Ge, G.; Han, D.; Lin, D.; Chu, W.; Sun, Y.; Jiang, L.; Ma, W.; Wang, C. MAC mode atomic force microscopy studies of living samples, ranging from cells to fresh tissue. *Ultramicroscopy* **2007**, *107*, 299–307. [[CrossRef](#)] [[PubMed](#)]
44. Mohn, F.; Schuler, B.; Gross, L.; Meyer, G. Different tips for high-resolution atomic force microscopy and scanning tunneling microscopy of single molecules. *Appl. Phys. Lett.* **2013**, *102*, 073109. [[CrossRef](#)]
45. Sahin, O.; Magonov, S.; Su, C.; Quate, C.F.; Solgaard, O. An atomic force microscope tip designed to measure time-varying nanomechanical forces. *Nat. Nanotechnol.* **2007**, *2*, 507–514. [[CrossRef](#)]
46. Senapati, S.; Manna, S.; Lindsay, S.; Zhang, P. Application of catalyst-free click reactions in attaching affinity molecules to tips of atomic force microscopy for detection of protein biomarkers. *Langmuir* **2013**, *29*, 14622–14630. [[CrossRef](#)]
47. Daza, R.; Colchero, L.; Corregidor, D.; Elices, M.; Guinea, G.V.; Rojo, F.J.; Pérez-Rigueiro, J. Functionalization of atomic force microscopy cantilevers and tips by activated vapour silanization. *Appl. Surf. Sci.* **2019**, *484*, 1141–1148. [[CrossRef](#)]
48. Girish, C.; Binulal, N.; Anitha, V.; Nair, S.; Mony, U.; Prasanth, R. Atomic force microscopic study of folate receptors in live cells with functionalized tips. *Appl. Phys. Lett.* **2009**, *95*, 223703. [[CrossRef](#)]
49. Lekka, M.; Gil, D.; Pogoda, K.; Dulińska-Litewka, J.; Jach, R.; Gostek, J.; Klymenko, O.; Prauzner-Bechcicki, S.; Stachura, Z.; Wiltowska-Zuber, J. Cancer cell detection in tissue sections using AFM. *Arch. Biochem. Biophys.* **2012**, *518*, 151–156. [[CrossRef](#)]
50. Lekka, M. Discrimination between normal and cancerous cells using AFM. *Bionanoscience* **2016**, *6*, 65–80. [[CrossRef](#)]

51. Schillers, H.; Rianna, C.; Schäpe, J.; Luque, T.; Doschke, H.; Wälte, M.; Uriarte, J.J.; Campillo, N.; Michanetzis, G.; Bobrowska, J. Standardized nanomechanical atomic force microscopy procedure (SNAP) for measuring soft and biological samples. *Sci. Rep.* **2017**, *7*, 1–9. [[CrossRef](#)] [[PubMed](#)]
52. Wang, B.; Xu, B. Transition model for ricin-aptamer interactions with multiple pathways and energy barriers. *Phys. Rev. E* **2014**, *89*, 022720. [[CrossRef](#)] [[PubMed](#)]
53. Wang, B.; Guo, C.; Chen, G.; Park, B.; Xu, B. Following aptamer–ricin specific binding by single molecule recognition and force spectroscopy measurements. *Chem. Commun.* **2012**, *48*, 1644–1646. [[CrossRef](#)] [[PubMed](#)]
54. Adams, J.D.; Erickson, B.W.; Grossenbacher, J.; Brugger, J.; Nievergelt, A.; Fantner, G.E. Harnessing the damping properties of materials for high-speed atomic force microscopy. *Nat. Nanotechnol.* **2016**, *11*, 147–151. [[CrossRef](#)]
55. Uchihashi, T.; Scheuring, S. Applications of high-speed atomic force microscopy to real-time visualization of dynamic biomolecular processes. *Biochim. Biophys. Acta (BBA)-Gen. Subj.* **2018**, *1862*, 229–240. [[CrossRef](#)]
56. Puppulin, L.; Kanayama, D.; Terasaka, N.; Sakai, K.; Kodera, N.; Umeda, K.; Sumino, A.; Marchesi, A.; Weilin, W.; Tanaka, H. Macrocytic Peptide-Conjugated Tip for Fast and Selective Molecular Recognition Imaging by High-Speed Atomic Force Microscopy. *ACS Appl. Mater. Interfaces* **2021**, *13*, 54817–54829. [[CrossRef](#)]
57. Yang, Q.; Ma, Q.; Herum, K.M.; Wang, C.; Patel, N.; Lee, J.; Wang, S.; Yen, T.M.; Wang, J.; Tang, H. Array atomic force microscopy for real-time multiparametric analysis. *Proc. Natl. Acad. Sci. USA* **2019**, *116*, 5872–5877. [[CrossRef](#)]
58. Park, B.; Lee, S.; Kwon, J.; Kim, W.; Jung, S.; Kim, C. Dual-pulse photoactivated atomic force microscopy. *Sci. Rep.* **2021**, *11*, 17097. [[CrossRef](#)]
59. Cheng, H.; Yu, J.; Wang, Z.; Ma, P.; Guo, C.; Wang, B.; Zhong, W.; Xu, B. Details of Single-Molecule Force Spectroscopy Data Decoded by a Network-Based Automatic Clustering Algorithm. *J. Phys. Chem. B* **2021**, *125*, 9660–9667. [[CrossRef](#)]
60. Creasey, R.; Sharma, S.; Gibson, C.T.; Craig, J.E.; Ebner, A.; Becker, T.; Hinterdorfer, P.; Voelcker, N.H. Atomic force microscopy-based antibody recognition imaging of proteins in the pathological deposits in pseudoexfoliation syndrome. *Ultramicroscopy* **2011**, *111*, 1055–1061. [[CrossRef](#)]
61. Best, R.B.; Li, B.; Steward, A.; Daggett, V.; Clarke, J. Can non-mechanical proteins withstand force? Stretching barnase by atomic force microscopy and molecular dynamics simulation. *Biophys. J.* **2001**, *81*, 2344–2356. [[CrossRef](#)]
62. Kawakami, M.; Smith, D. A new atomic force microscope force ramp technique using digital force feedback control reveals mechanically weak protein unfolding events. *Nanotechnology* **2008**, *19*, 495704. [[CrossRef](#)]
63. Peng, Q.; Li, H. Atomic force microscopy reveals parallel mechanical unfolding pathways of T4 lysozyme: Evidence for a kinetic partitioning mechanism. *Proc. Natl. Acad. Sci. USA* **2008**, *105*, 1885–1890. [[CrossRef](#)]
64. Mahmood, I.A.; Moheimani, S.R.; Bhikkaji, B. A new scanning method for fast atomic force microscopy. *IEEE Trans. Nanotechnol.* **2009**, *10*, 203–216. [[CrossRef](#)]
65. Hansma, H.G.; Bezanilla, M.; Zenhausern, F.; Adrian, M.; Sinsheimer, R.L. Atomic force microscopy of DNA in aqueous solutions. *Nucleic Acids Res.* **1993**, *21*, 505–512. [[CrossRef](#)]
66. Zhu, R.; Howorka, S.; Pröll, J.; Kienberger, F.; Preiner, J.; Hesse, J.; Ebner, A.; Pastushenko, V.P.; Gruber, H.J.; Hinterdorfer, P. Nanomechanical recognition measurements of individual DNA molecules reveal epigenetic methylation patterns. *Nat. Nanotechnol.* **2010**, *5*, 788–791. [[CrossRef](#)]
67. Shim, W.C.; Woo, S.; Park, J.W. Nanoscale Force-Mapping-Based Quantification of Low-Abundance Methylated DNA. *Nano Lett.* **2022**, *22*, 1324–1330. [[CrossRef](#)]
68. Strobl, K.; Mateu, M.; de Pablo, P.J. Exploring nucleic acid condensation and release from individual parvovirus particles with different physicochemical cues. *Virology* **2023**, *581*, 1–7. [[CrossRef](#)]
69. Abu-Lail, N.; Camesano, T. Polysaccharide properties probed with atomic force microscopy. *J. Microsc.* **2003**, *212*, 217–238. [[CrossRef](#)]
70. Guo, C.; Fan, X.; Qiu, H.; Xiao, W.; Wang, L.; Xu, B. High-resolution probing heparan sulfate–antithrombin interaction on a single endothelial cell surface: Single-molecule AFM studies. *Phys. Chem. Chem. Phys.* **2015**, *17*, 13301–13306. [[CrossRef](#)]
71. Li, M.; Xi, N.; Wang, Y.; Liu, L. Nanoscale multiparametric imaging of peptide-assembled nanofibrillar hydrogels by atomic force microscopy. *IEEE Trans. Nanotechnol.* **2019**, *18*, 315–328. [[CrossRef](#)]
72. Gaspar, D.; Freire, J.M.; Pacheco, T.R.; Barata, J.T.; Castanho, M.A. Apoptotic human neutrophil peptide-1 anti-tumor activity revealed by cellular biomechanics. *Biochim. Biophys. Acta (BBA)-Mol. Cell Res.* **2015**, *1853*, 308–316. [[CrossRef](#)] [[PubMed](#)]
73. Zhang, Y.; Zhang, M.; Alexander Reese, R.; Zhang, H.; Xu, B. Real-time single molecular study of a pretreated cellulose hydrolysis mode and individual enzyme movement. *Biotechnol. Biofuels* **2016**, *9*, 1–12. [[CrossRef](#)] [[PubMed](#)]
74. Zhang, M.; Wu, S.-C.; Zhou, W.; Xu, B. Imaging and measuring single-molecule interaction between a carbohydrate-binding module and natural plant cell wall cellulose. *J. Phys. Chem. B* **2012**, *116*, 9949–9956. [[CrossRef](#)] [[PubMed](#)]
75. Zhang, M.; Wang, B.; Xu, B. Measurements of single molecular affinity interactions between carbohydrate-binding modules and crystalline cellulose fibrils. *Phys. Chem. Chem. Phys.* **2013**, *15*, 6508–6515. [[CrossRef](#)]
76. Zhang, M.; Wang, B.; Xu, B. Mapping single molecular binding kinetics of carbohydrate-binding module with crystalline cellulose by atomic force microscopy recognition imaging. *J. Phys. Chem. B* **2014**, *118*, 6714–6720. [[CrossRef](#)]
77. Kolodziejczyk, A.; Jakubowska, A.; Kucinska, M.; Wasiaik, T.; Komorowski, P.; Makowski, K.; Walkowiak, B. Sensing of silver nanoparticles on/in endothelial cells using atomic force spectroscopy. *J. Mol. Recognit.* **2018**, *31*, e2723. [[CrossRef](#)]
78. Dong, M.; Sahin, O. A nanomechanical interface to rapid single-molecule interactions. *Nat. Commun.* **2011**, *2*, 247. [[CrossRef](#)]

79. Browning-Kelley, M.; Wadu-Mesthrige, K.; Hari, V.; Liu, G. Atomic force microscopic study of specific antigen/antibody binding. *Langmuir* **1997**, *13*, 343–350. [[CrossRef](#)]
80. Hu, J.; Gao, M.; Wang, Z.; Chen, Y.; Song, Z.; Xu, H. Direct imaging of antigen–antibody binding by atomic force microscopy. *Appl. Nanosci.* **2021**, *11*, 293–300. [[CrossRef](#)]
81. Hinterdorfer, P.; Baumgartner, W.; Gruber, H.J.; Schilcher, K.; Schindler, H. Detection and localization of individual antibody–antigen recognition events by atomic force microscopy. *Proc. Natl. Acad. Sci. USA* **1996**, *93*, 3477–3481. [[CrossRef](#)] [[PubMed](#)]
82. Berquand, A.; Xia, N.; Castner, D.G.; Clare, B.H.; Abbott, N.L.; Dupres, V.; Adriaensen, Y.; Dufrène, Y.F. Antigen binding forces of single antilysozyme Fv fragments explored by atomic force microscopy. *Langmuir* **2005**, *21*, 5517–5523. [[CrossRef](#)] [[PubMed](#)]
83. Kienberger, F.; Kada, G.; Mueller, H.; Hinterdorfer, P. Single molecule studies of antibody–antigen interaction strength versus intra-molecular antigen stability. *J. Mol. Biol.* **2005**, *347*, 597–606. [[CrossRef](#)] [[PubMed](#)]
84. Chen, Y.; Zeng, G.; Chen, S.S.; Feng, Q.; Chen, Z.W. AFM force measurements of the gp120–sCD4 and gp120 or CD4 antigen–antibody interactions. *Biochem. Biophys. Res. Commun.* **2011**, *407*, 301–306. [[CrossRef](#)]
85. Hianik, T. Aptamer-based biosensors. In *Encyclopedia of Interfacial Chemistry*; Wandelt, K., Ed.; Elsevier: Cambridge, MA, USA, 2018; Volume 7, pp. 11–19.
86. Wang, C.; Yadavalli, V.K. Spatial recognition and mapping of proteins using DNA aptamers. *Nanotechnology* **2014**, *25*, 455101. [[CrossRef](#)]
87. Junior, B.B.; Batistuti, M.R.; Pereira, A.S.; de Sousa Russo, E.M.; Mulato, M. Electrochemical aptasensor for NS1 detection: Towards a fast dengue biosensor. *Talanta* **2021**, *233*, 122527. [[CrossRef](#)]
88. Leitner, M.; Poturnayova, A.; Lamprecht, C.; Weich, S.; Snejdarkova, M.; Karpisova, I.; Hianik, T.; Ebner, A. Characterization of the specific interaction between the DNA aptamer sgc8c and protein tyrosine kinase-7 receptors at the surface of T-cells by biosensing AFM. *Anal. Bioanal. Chem.* **2017**, *409*, 2767–2776. [[CrossRef](#)]
89. Poturnayová, A.; Buriková, M.; Bízik, J.; Hianik, T. DNA aptamers in the detection of leukemia cells by the thickness shear mode acoustics method. *ChemPhysChem* **2019**, *20*, 545–554. [[CrossRef](#)]
90. van Galen, M.; Kaniraj, J.P.; Albada, B.; Sprakel, J. Single-Molecule Force Spectroscopy of a Tetraaryl Succinonitrile Mechanophore. *J. Phys. Chem. C* **2022**, *126*, 1215–1221. [[CrossRef](#)]
91. Qin, C.; Clarke, K.; Li, K. Interactive forces between lignin and cellulase as determined by atomic force microscopy. *Biotechnol. Biofuels* **2014**, *7*, 1–10. [[CrossRef](#)]
92. Kim, D.; Sahin, O. Imaging and three-dimensional reconstruction of chemical groups inside a protein complex using atomic force microscopy. *Nat. Nanotechnol.* **2015**, *10*, 264–269. [[CrossRef](#)]
93. Viani, M.B.; Pietrasanta, L.I.; Thompson, J.B.; Chand, A.; Gebeshuber, I.C.; Kindt, J.H.; Richter, M.; Hansma, H.G.; Hansma, P.K. Probing protein–protein interactions in real time. *Nat. Struct. Biol.* **2000**, *7*, 644–647. [[CrossRef](#)]
94. Zapotoczny, B.; Braet, F.; Wisse, E.; Lekka, M.; Szymonski, M. Biophysical nanocharacterization of liver sinusoidal endothelial cells through atomic force microscopy. *Biophys. Rev.* **2020**, *12*, 625–636. [[CrossRef](#)]
95. Bonanni, B.; Kamruzzahan, A.; Bizzarri, A.; Rankl, C.; Gruber, H.; Hinterdorfer, P.; Cannistraro, S. Single molecule recognition between cytochrome C 551 and gold-immobilized azurin by force spectroscopy. *Biophys. J.* **2005**, *89*, 2783–2791. [[CrossRef](#)]
96. Sanchez, H.; Suzuki, Y.; Yokokawa, M.; Takeyasu, K.; Wyman, C. Protein–DNA interactions in high speed AFM: Single molecule diffusion analysis of human RAD54. *Integr. Biol.* **2011**, *3*, 1127–1134. [[CrossRef](#)]
97. Touhami, A.; Hoffmann, B.; Vasella, A.; Denis, F.A.; Dufrène, Y.F. Probing specific lectin–carbohydrate interactions using atomic force microscopy imaging and force measurements. *Langmuir* **2003**, *19*, 1745–1751. [[CrossRef](#)]
98. Zhang, M.; Chen, G.; Kumar, R.; Xu, B. Mapping out the structural changes of natural and pretreated plant cell wall surfaces by atomic force microscopy single molecular recognition imaging. *Biotechnol. Biofuels* **2013**, *6*, 147. [[CrossRef](#)]
99. Faria, E.C.; Ma, N.; Gazi, E.; Gardner, P.; Brown, M.; Clarke, N.W.; Snook, R.D. Measurement of elastic properties of prostate cancer cells using AFM. *Analyst* **2008**, *133*, 1498–1500. [[CrossRef](#)]
100. Li, M.; Liu, L.; Xi, N.; Wang, Y.; Dong, Z.; Xiao, X.; Zhang, W. Atomic force microscopy imaging and mechanical properties measurement of red blood cells and aggressive cancer cells. *Sci. China Life Sci.* **2012**, *55*, 968–973. [[CrossRef](#)]
101. Ansardamavandi, A.; Tafazzoli-Shadpour, M.; Omidvar, R.; Nili, F. An AFM-based nanomechanical study of ovarian tissues with pathological conditions. *Int. J. Nanomed.* **2020**, 4333–4350. [[CrossRef](#)]
102. Giannetti, A.; Revilloud, J.; Verdier, C. Mechanical properties of 3D tumor spheroids measured by AFM. *Comput. Methods Biomech. Biomed. Eng.* **2020**, *23*, S125–S127. [[CrossRef](#)]
103. Lekka, M.; Fornal, M.; Pyka-Fościak, G.; Lebed, K.; Wizner, B.; Grodzicki, T.; Styczeń, J. Erythrocyte stiffness probed using atomic force microscope. *Biorheology* **2005**, *42*, 307–317. [[PubMed](#)]
104. Li, M.; Liu, L.; Xi, N.; Wang, Y.; Dong, Z.; Li, G.; Xiao, X.; Zhang, W. Measuring the physical properties of the lymphoma cells using atomic force microscopy. In Proceedings of the 2010 IEEE Nanotechnology Materials and Devices Conference, Monterey, CA, USA, 12–15 October 2010; pp. 310–314.
105. Haase, K.; Pelling, A.E. Investigating cell mechanics with atomic force microscopy. *J. R. Soc. Interface* **2015**, *12*, 20140970. [[CrossRef](#)] [[PubMed](#)]
106. Wang, B.; Park, B.; Kwon, Y.; Xu, B. Determining the elastic properties of aptamer–ricin single molecule multiple pathway interactions. *Appl. Phys. Lett.* **2014**, *104*, 193702. [[CrossRef](#)]

107. Li, M.; Liu, L.; Xiao, X.; Xi, N.; Wang, Y. Effects of methotrexate on the viscoelastic properties of single cells probed by atomic force microscopy. *J. Biol. Phys.* **2016**, *42*, 551–569. [[CrossRef](#)]
108. Wei, F.; Yang, H.; Liu, L.; Li, G. A novel approach for extracting viscoelastic parameters of living cells through combination of inverse finite element simulation and Atomic Force Microscopy. *Comput. Methods Biomech. Biomed. Eng.* **2017**, *20*, 373–384. [[CrossRef](#)]
109. Li, Q.; Lee, G.Y.; Ong, C.N.; Lim, C.T. AFM indentation study of breast cancer cells. *Biochem. Biophys. Res. Commun.* **2008**, *374*, 609–613. [[CrossRef](#)]
110. Xu, W.; Mezencev, R.; Kim, B.; Wang, L.; McDonald, J.; Sulchek, T. Cell stiffness is a biomarker of the metastatic potential of ovarian cancer cells. *PLoS One* **2012**, *7*, e46609. [[CrossRef](#)]
111. Li, M.; Xiao, X.; Liu, L.; Xi, N.; Wang, Y. Rapid recognition and functional analysis of membrane proteins on human cancer cells using atomic force microscopy. *J. Immunol. Methods* **2016**, *436*, 41–49. [[CrossRef](#)]
112. Paul, D.; Roy, A.; Nandy, A.; Datta, B.; Borar, P.; Pal, S.K.; Senapati, D.; Rakshit, T. Identification of biomarker hyaluronan on colon cancer extracellular vesicles using correlative AFM and spectroscopy. *J. Phys. Chem. Lett.* **2020**, *11*, 5569–5576. [[CrossRef](#)]
113. Park, K.; Lonsberry, G.E.; Gearing, M.; Levey, A.I.; Desai, J.P. Viscoelastic properties of human autopsy brain tissues as biomarkers for Alzheimer's diseases. *IEEE Trans. Biomed. Eng.* **2018**, *66*, 1705–1713. [[CrossRef](#)]
114. Nirmalraj, P.N.; Schneider, T.; Felbecker, A. Spatial organization of protein aggregates on red blood cells as physical biomarkers of Alzheimer's disease pathology. *Sci. Adv.* **2021**, *7*, eabj2137. [[CrossRef](#)]
115. Strijkova-Kenderova, V.; Todinova, S.; Andreeva, T.; Bogdanova, D.; Langari, A.; Danailova, A.; Krumova, S.; Zlatareva, E.; Kalaydzhev, N.; Milanov, I. Morphometry and stiffness of red blood cells—Signatures of neurodegenerative diseases and aging. *Int. J. Mol. Sci.* **2022**, *23*, 227. [[CrossRef](#)]
116. Patil, S.; Martinez, N.F.; Lozano, J.R.; Garcia, R. Force microscopy imaging of individual protein molecules with sub-pico Newton force sensitivity. *J. Mol. Recognit. Interdiscip. J.* **2007**, *20*, 516–523. [[CrossRef](#)]
117. Gilbert, Y.; Deghorain, M.; Wang, L.; Xu, B.; Pollheimer, P.D.; Gruber, H.J.; Errington, J.; Hallet, B.; Haulot, X.; Verbelen, C. Single-molecule force spectroscopy and imaging of the vancomycin/D-Ala-D-Ala interaction. *Nano Lett.* **2007**, *7*, 796–801. [[CrossRef](#)]
118. Rankl, C.; Kienberger, F.; Wildling, L.; Wruss, J.; Gruber, H.J.; Blaas, D.; Hinterdorfer, P. Multiple receptors involved in human rhinovirus attachment to live cells. *Proc. Natl. Acad. Sci. USA* **2008**, *105*, 17778–17783. [[CrossRef](#)]
119. Fantner, G.E.; Barbero, R.J.; Gray, D.S.; Belcher, A.M. Kinetics of antimicrobial peptide activity measured on individual bacterial cells using high-speed atomic force microscopy. *Nat. Nanotechnol.* **2010**, *5*, 280–285. [[CrossRef](#)]
120. Faustino, A.F.; Carvalho, F.A.; Martins, I.C.; Castanho, M.A.; Mohana-Borges, R.; Almeida, F.C.; Da Poian, A.T.; Santos, N.C. Dengue virus capsid protein interacts specifically with very low-density lipoproteins. *Nanomed. Nanotechnol. Biol. Med.* **2014**, *10*, 247–255. [[CrossRef](#)]
121. Herman-Bausier, P.; Dufrière, Y.F. Atomic force microscopy reveals a dual collagen-binding activity for the staphylococcal surface protein SdrF. *Mol. Microbiol.* **2016**, *99*, 611–621. [[CrossRef](#)]
122. Newton, R.; Delguste, M.; Koehler, M.; Dumitru, A.C.; Laskowski, P.R.; Müller, D.J.; Alsteens, D. Combining confocal and atomic force microscopy to quantify single-virus binding to mammalian cell surfaces. *Nat. Protoc.* **2017**, *12*, 2275–2292. [[CrossRef](#)]
123. Kiss, B.; Kis, Z.; Pályi, B.; Kellermayer, M.S. Topography, spike dynamics, and nanomechanics of individual native SARS-CoV-2 virions. *Nano Lett.* **2021**, *21*, 2675–2680. [[CrossRef](#)] [[PubMed](#)]
124. Xing, X.; Jin, H.; Lu, Y.; Wang, Q.; Pan, Y.; Cai, J.; Wang, H. Detection of erythrocytes in patient with elliptocytosis complicating ITP using atomic force microscopy. *Micron* **2011**, *42*, 42–46. [[CrossRef](#)] [[PubMed](#)]
125. Carvalho, F.A.; Connell, S.; Miltenberger-Miltenyi, G.; Pereira, S.V.; Tavares, A.; Ariëns, R.A.; Santos, N.C. Atomic force microscopy-based molecular recognition of a fibrinogen receptor on human erythrocytes. *ACS Nano* **2010**, *4*, 4609–4620. [[CrossRef](#)] [[PubMed](#)]
126. Liu, J.; Li, J. Detection of erythrocytes in patients with Waldenström macroglobulinemia using atomic force microscopy. *Acta Biochim. Biophys. Sin.* **2014**, *46*, 420–425. [[CrossRef](#)]
127. Li, M.; Liu, L.; Xiao, X.; Xi, N.; Wang, Y. Viscoelastic properties measurement of human lymphocytes by atomic force microscopy based on magnetic beads cell isolation. *IEEE Trans. NanoBiosci.* **2016**, *15*, 398–411. [[CrossRef](#)]
128. Jazvinšćak Jembrek, M.; Vlanić, J.; Čadež, V.; Šegota, S. Atomic force microscopy reveals new biophysical markers for monitoring subcellular changes in oxidative injury: Neuroprotective effects of quercetin at the nanoscale. *PLoS ONE* **2018**, *13*, e0200119. [[CrossRef](#)]
129. Feng, Y.; Liu, M.; Li, X.; Li, M.; Xing, X.; Liu, L. Nanomechanical signatures of extracellular vesicles from hematologic cancer patients unraveled by atomic force microscopy for liquid biopsy. *Nano Lett.* **2023**, *23*, 1591–1599. [[CrossRef](#)]
130. Zhang, G.; Wang, L.; Pan, J. Probing the binding of the flavonoid diosmetin to human serum albumin by multispectroscopic techniques. *J. Agric. Food Chem.* **2012**, *60*, 2721–2729. [[CrossRef](#)]
131. Domingues, M.M.; Silva, P.M.; Franquelim, H.G.; Carvalho, F.A.; Castanho, M.A.; Santos, N.C. Antimicrobial protein rBPI21-induced surface changes on Gram-negative and Gram-positive bacteria. *Nanomed. Nanotechnol. Biol. Med.* **2014**, *10*, 543–551. [[CrossRef](#)]

132. Rajendran, A.; Endo, M.; Hidaka, K.; Teulade-Fichou, M.-P.; Mergny, J.-L.; Sugiyama, H. Small molecule binding to a G-hairpin and a G-triplex: A new insight into anticancer drug design targeting G-rich regions. *Chem. Commun.* **2015**, *51*, 9181–9184. [[CrossRef](#)]
133. Li, M.; Xiao, X.; Liu, L.; Xi, N.; Wang, Y. Nanoscale quantifying the effects of targeted drug on chemotherapy in lymphoma treatment using atomic force microscopy. *IEEE Trans. Biomed. Eng.* **2015**, *63*, 2187–2199. [[CrossRef](#)]
134. Ren, J.; Huang, H.; Liu, Y.; Zheng, X.; Zou, Q. An atomic force microscope study revealed two mechanisms in the effect of anticancer drugs on rate-dependent Young's modulus of human prostate cancer cells. *PLoS ONE* **2015**, *10*, e0126107. [[CrossRef](#)]
135. Alhalhooly, L.; Mamnoon, B.; Kim, J.; Mallik, S.; Choi, Y. Dynamic cellular biomechanics in responses to chemotherapeutic drug in hypoxia probed by atomic force spectroscopy. *Oncotarget* **2021**, *12*, 1165. [[CrossRef](#)]
136. Taranta, M.; Bizzarri, A.R.; Cannistraro, S. Probing the interaction between p53 and the bacterial protein azurin by single molecule force spectroscopy. *J. Mol. Recognit. Interdiscip. J.* **2008**, *21*, 63–70. [[CrossRef](#)]
137. Zhang, J.; Wu, G.; Song, C.; Li, Y.; Qiao, H.; Zhu, P.; Hinterdorfer, P.; Zhang, B.; Tang, J. Single molecular recognition force spectroscopy study of a luteinizing hormone-releasing hormone analogue as a carcinoma target drug. *J. Phys. Chem. B* **2012**, *116*, 13331–13337. [[CrossRef](#)]
138. Xiao, H.; Zhang, J.; Xu, Z.; Feng, Y.; Zhang, M.; Liu, J.; Chen, R.; Shen, J.; Wu, J.; Lu, Z. Metformin is a novel suppressor for transforming growth factor (TGF)- $\beta$ 1. *Sci. Rep.* **2016**, *6*, 28597. [[CrossRef](#)]
139. Li, M.; Liu, L.; Xiao, X.; Xi, N.; Wang, Y. The dynamic interactions between chemotherapy drugs and plasmid DNA investigated by atomic force microscopy. *Sci. China Mater.* **2017**, *3*, 269–278. [[CrossRef](#)]
140. Yun, X.; Tang, M.; Yang, Z.; Wilksch, J.J.; Xiu, P.; Gao, H.; Zhang, F.; Wang, H. Interrogation of drug effects on HeLa cells by exploiting new AFM mechanical biomarkers. *RSC Adv.* **2017**, *7*, 43764–43771. [[CrossRef](#)]
141. Song, G.; Tian, F.; Liu, H.; Li, G.; Zheng, P. Pioglitazone inhibits metal cluster transfer of mitoNEET by stabilizing the labile Fe–N bond revealed at single-bond level. *J. Phys. Chem. Lett.* **2021**, *12*, 3860–3867. [[CrossRef](#)]

**Disclaimer/Publisher's Note:** The statements, opinions and data contained in all publications are solely those of the individual author(s) and contributor(s) and not of MDPI and/or the editor(s). MDPI and/or the editor(s) disclaim responsibility for any injury to people or property resulting from any ideas, methods, instructions or products referred to in the content.